



# Trend detection in surface air temperature in Ontario and Quebec, Canada during 1967–2006 using the discrete wavelet transform



D. Nalley<sup>a</sup>, J. Adamowski<sup>a,\*</sup>, B. Khalil<sup>a</sup>, B. Ozga-Zielinski<sup>b</sup>

<sup>a</sup> Department of Bioresource Engineering, Faculty of Agriculture and Environmental Sciences, McGill University, Ste-Anne-de-Bellevue, Quebec H9X 3V9, Canada

<sup>b</sup> Department of Environment Protection and Development, Environmental Engineering Faculty, Warsaw University of Technology, ul. Nowowiejska 20, Warsaw 00-653, Poland

## ARTICLE INFO

### Article history:

Received 3 April 2013

Received in revised form 29 June 2013

Accepted 30 June 2013

### Keywords:

Temperature

Trend

Climate change

Discrete wavelet transform

Mann–Kendall trend test

Canada

## ABSTRACT

The main purpose of this study is to detect trends in the mean surface air temperature over the southern parts of Ontario and Quebec, Canada, for the period of 1967–2006. This is accomplished by determining the most dominant periodic components that affect trends in different temperature data categories (monthly, seasonally-based, seasonal, and annual), which were obtained from a total of five stations. The discrete wavelet transform (DWT) technique, the Mann–Kendall (MK) trend test, and sequential Mann–Kendall analysis were used in this study – co-utilizing these techniques in temperature trend studies has not been explored extensively. The mother wavelet, number of decomposition levels, and boundary condition were determined using a newly proposed criterion based on the relative error of the MK Z-values between the original data and the approximation component of the last decomposition level. This study found that all stations experienced positive trends: significant trends were observed in all of the monthly, seasonally-based, and annual data. For the different seasons, although the trend values were all positive, not all stations experienced significant trends. It was found that high-frequency components ranging from 2 to 12 months were more prominent for trends in the higher resolution data (i.e. monthly and seasonally based). The positive trends observed for the annual data are thought to be mostly attributable to warming during winter and summer seasons, which are manifested in the form of multiyear to decadal events (mostly between 8 and 16 years).

© 2013 Elsevier B.V. All rights reserved.

## 1. Introduction

The impacts of climate variability can be assessed by analyzing trends in surface air temperature. According to the latest assessment report by the IPCC (IPCC, 2007), mean global surface air temperature has experienced an increase of between 0.56 °C and 0.92 °C for the period from 1906 to 2005. Changes in surface air temperature as a result of

changing climate have serious ramifications on the hydrological cycle (and therefore, on water resources) and the surface energy budget (Vincent et al., 2007). Examples of these consequences are: intensification of the hydrological cycle (Mishra and Singh, 2010), modification of hydrological indicators such as seasonal runoff, precipitation, streamflow, and potential evapotranspiration (Mimikou et al., 2000; Labat et al., 2004), more severe flood discharges (Ludwig et al., 2004), sea-level rise (which has serious implications on the economy and societies in general) (Nicholls and Tol, 2006), and increased risks of health-related problems (Karaburun et al., 2011), etc.

Since climate change is directly linked to temperature, a large number of studies have been undertaken globally and

\* Corresponding author at: Department of Bioresource Engineering, Faculty of Agricultural and Environmental Sciences, McGill University, Ste-Anne-de-Bellevue, Quebec H9X3V9, Canada. Tel.: +1 514 224 0492.

E-mail addresses: [deasy.nalley@mail.mcgill.ca](mailto:deasy.nalley@mail.mcgill.ca) (D. Nalley), [jan.adamowski@mcgill.ca](mailto:jan.adamowski@mcgill.ca) (J. Adamowski), [bahaa.e.khalil@mail.mcgill.ca](mailto:bahaa.e.khalil@mail.mcgill.ca) (B. Khalil).

regionally in order to assess temperature trends and to quantify the impacts of increasing temperature. Most of these studies have found the existence of positive trends in different temperature indices. For example, Shrestha et al. (1999) found that the temperature patterns in Nepal were increasing after 1977, with a rate ranging from 0.03 to 0.12 °C per year. Domroes and El-Tantawi (2005) reported increasing mean temperature trends in northern Egypt over the period 1941–2000. Fan and Wang (2011) studied climate change by looking at the monotonic trends in annual and seasonal air temperature indices across Shanxi province in China, and found that there have been warming trends in temperature over the period 1959–2008. Karaburun et al. (2011) also analyzed the spatio-temporal patterns of temperature change in Istanbul, Turkey for the period of 1975 to 2006, and observed that warmer temperature trends generally prevailed for seasonal and annual temperature indices. Although many studies have found that all seasons showed positive trends, winter usually experiences the greatest warming (e.g. Lund et al., 2001; Rebetez and Reinhard, 2007; Fan and Wang, 2011). Fan and Wang (2011) observed that winter warming in Shanxi province in China was statistically significant at less than the 0.1% significance level. Rebetez and Reinhard (2007) also found that the greatest warming occurred during winter (1975–2004) in Switzerland.

It has been mentioned that the northern hemisphere has been experiencing more temperature warming since the 1950s compared to the southern hemispheres (Jones and Moberg, 2003; IPCC, 2007; Chaouche et al., 2010; Karaburun et al., 2011). More specifically, North America is expected to experience a warmer climate, in which the increase in the mean annual temperature could be more than that of the global mean increase (IPCC, 2007). Moberg et al. (2005) reconstructed long-term proxy data from tree-ring and sediments in lakes and oceans to analyze the variation in temperature in the northern hemisphere. They found that there has never been any period within the past 2000 years that is as warm as post 1990 (Moberg et al., 2005). Lund et al. (2001) and Lu et al. (2005) also found that there were increasing temperature trends during 1922–2000 in the East, West-Coast, and northern Midwest of the USA. All seasons in the contiguous 48 states experienced increasing temperature trends with winter showing the highest warming (Lu et al., 2005).

Zhang et al. (2000) mentioned that it may be easier to assess climate change in countries such as Canada because according to Nicholls et al. (1996), human-induced climate change is foreseen to be more severe in high-latitude areas. As such, numerous studies on trends of Canadian temperature indices have been conducted both at the national and regional levels. Zhang et al. (2000) provided comprehensive information on Canada's temperature and precipitation trends. At the national level it was found that the annual mean temperature has experienced an increase of approximately 1 °C during the last half of the 20th century (Zhang et al., 2000). For areas below 60°N, Zhang et al. (2000) showed that although the trends are not monotonic during 1900–1998 and differed from region to region, there is a statistically significant increase in the mean annual temperature that was caused by the increases before the 1940s and after the 1970s. Mohsin and Gough (2010) analyzed the temperature trends in a smaller spatial scale covering Toronto and the Greater Toronto area for the period 1970–2000. The trend analysis on the annual minimum

and mean temperature indices showed that urbanization has contributed to the observed warming trend experienced by the urban stations (Toronto Pearson exhibited the highest warming trend). Similarly, Prokoph and Patterson (2004) and Adamowski and Prokoph (2013) found that the temperature in urban Ottawa was going up by more than 0.01 °C per year compared to the nearby rural areas over the past 100 years, which was associated with the population growth and urban heat island effects.

Studies investigating trends in temperature commonly involve the use of the Mann–Kendall (MK) trend test. This trend test is usually preferred over other statistical tests because of its robustness and power. The MK test may be used even if the analyzed data does not follow a Gaussian normal frequency distribution (Kadioğlu, 1997). Chaouche et al. (2010) chose to employ the MK test in studying climatic indices (including temperature) in the context of climate change because trends are assumed to be slowly changing phenomena; they also mentioned that even if a break change occurs, the MK test is still powerful. Having said this, the use of the original MK test only gives accurate results when the test is applied on data that are free from serial correlation (Mohsin and Gough, 2010). Hirsch and Slack (1984) and Hamed and Rao (1998) proposed modifications to the original MK test in order to account for seasonality and serial correlation factors that may be present in a time series.

When analyzing temperature time series, it is important to examine the behavior of the different low- and high-frequency components contained in the data, which represent fluctuations such as inter-annual and decadal events (Baliunas et al., 1997). Detecting and identifying trends in non-stationary temperature datasets is complicated due to factors such as changes in climate that occur in non-monotonic and non-uniform fashions. Additionally, variability and trends that are observed in a dataset can be associated with climate noise (Franzke, 2010). Trends in temperature can also be enhanced or reduced by the variability in the temperature itself (that may occur in the form of different time scales) and changes in climate that occur naturally. Prior to computing a trend assessment, it is important to define what a trend is. Since many climate data exhibit nonlinear and non-stationary characteristics, commonly defined trends using a simple straight line fit on to the data are not suitable (Wu et al., 2007). Analyzing temperature trends that involves the use of methods such as moving average, regression analysis, and Fourier-based techniques may not also be appropriate because of their assumptions that involve stationary and linear inferences (Wu et al., 2007).

A spectral analysis method that has been found to be very useful for analyzing geophysical time series (which are often characterized by non-stationarity) is the wavelet transform (WT) (Lau and Weng, 1995; Lindsay et al., 1996). The WT is suitable for decomposing one-dimensional non-stationary time series into its two-dimensional (time-frequency) information (Lau and Weng, 1995; Torrence and Compo, 1998; Pišoft et al., 2004). In this study, the non-linear trends are assumed to have occurred in a gradual manner and are contained in the low-frequency components of the data.

Numerous studies have acknowledged that the WT is superior for use in analyzing non-stationary data compared to conventional spectral analysis methods, such as the Fourier transform (FT). The FT decomposes signals into sine wave

functions, which have unlimited duration, whereas the WT – having an irregular and non-symmetrical function shape – decomposes signals into wavelet functions that have limited duration and zero mean (Drago and Boxall, 2002). The WT was used to separate the high-frequency components and low-frequency components of the temperature data used in this study. The last decomposition level contains the lowest-frequency component of the analyzed temperature data, which represents the trend component of the data. The different decomposition levels – which represent different periodic time scales – were analyzed for trends. The goal was to then determine the most important periodic components that affect the observed temperature trends. This was accomplished by using the MK test (and its sequential version) to evaluate the behavior of the different periodic components resulting from the DWT which range from intra-annual to decadal time scales. Lower periodic components may be related to factors such as seasonality, which can be reflected in the form of semi-annual and annual cycles. Large-scale climate circulations, some of which tend to occur in a long time-scale and are thus associated with higher decomposition levels or periodic components. For example, if 11-year or 22-year periodic oscillations are present and found to be important in the spectrum of a climate data analysis, they may be related to the Sun's activity cycles: the 11-year sunspot cycle and the 22-year solar magnetic cycle.

The use of WT has been seen in several climatological applications, including studies of spatiotemporal patterns of temperature changes. Baliunas et al. (1997) employed the WT in order to analyze temperature trends and their time-scale information in central England. The 7.5-year scale was observed to be the most stable peak within the 2- to 105-year time-scale range (Baliunas et al., 1997). Pišoft et al. (2004) were able to demonstrate that the global wavelet spectrum of the continuous wavelet transform (CWT) had better accuracy in determining the years of local maxima for the longest time periods of the studied Czech temperature series compared to the FT – the wavelet power was able to reveal different features and activities of each periodic component. Similarly, Jung et al. (2002) and Prokoph and Patterson (2004) utilized the CWT to analyze the warming trends in the winter temperature data in South Korea and Ottawa, respectively. The results of the WA for the winter temperature over South Korea revealed that the decadal and inter-decadal events of 16 and 33 years were strongly persistent during 1954–1999 (Jung et al., 2002). A slightly weaker inter-annual event of 4.9 years was found to be associated with the El Niño cycle (Jung et al., 2002). The results of CWT in studying urban warming trends in Ottawa, Ontario revealed that multi-decadal and inter-seasonal periodic modes are thought to contribute to the winter warming in Ottawa, which is related to the urban heat island (Prokoph and Patterson, 2004; Adamowski and Prokoph, 2013).

The majority of studies that employed WT in investigating trends in temperature used the CWT approach (e.g. Baliunas et al., 1997; Jung et al., 2002; Polyakov et al., 2003; Pišoft et al., 2004; Prokoph and Patterson, 2004; and Kravchenko et al., 2011). This is due to the fact that the CWT allows for the analysis of data at all locations of time and space (Wang and Lu, 2009). However, rather than producing a one-dimensional time series, CWT produces a two-dimensional scalogram, which may contain redundant information (Percival, 2008).

Furthermore, edge effects associated with the application of the CWT complicate signal reconstructions (Adamowski et al., 2009). If the discrete wavelet transform (DWT) approach is chosen, the decomposition process is simplified but still efficient because the computation is based on a dyadic discretization (integer powers of two) (Chou, 2007). This generates a compact representation of the analyzed signal (Wang and Lu, 2009) and thus, the redundancy of the information is reduced. Achieving perfect signal reconstructions is also relatively simple when the DWT approach is used.

The main purpose of this study is to analyze trends in four temperature categories – monthly, seasonally-based, seasonal, and annual – by combining the use of the DWT approach with the MK trend test. The DWT is used to decompose the time series into their different lower-resolution components; the MK test was applied to each time series resulting from the decomposition in order to assess their statistical significance. The dyadic arrangement used in the DWT procedure allowed us to investigate the contributions of periodic events – ranging from 2 months to 32 years – to the observed trends over the 40-year study period. Although there are many temperature trend detection studies that have been conducted in Canada, these studies have not explored the contribution of the high- and low-frequency components of the analyzed data to the observed trends using the DWT and the MK trend test. Additionally, temperature trend studies that focus on localized areas in Canada are still relatively rare.

## 2. Theoretical background

### 2.1. Time-scale representation of signals by the wavelet transform (WT)

The wavelet transform is a mathematical tool that uses wave functions – known as wavelets – similar to sine and cosine functions. A wavelet must satisfy the admissibility condition of having a zero mean (Farge, 1992; Torrence and Compo, 1998). The property of the WT in which it is localized in time and frequency domains is very useful because it allows for the extraction of the different modes of variability that vary in time (Lim and Lye, 2004). The window used in the WT can be adjusted to the whole time-frequency domain – it can be dilated and shifted with a resolution that is adjustable in both time and frequency domains (Lau and Weng, 1995). The narrow and wide windows are used to capture the high-frequency and low-frequency components of the signal, respectively (Lau and Weng, 1995). Therefore, when analyzing a signal, WT separates the signal's high frequency (short periodic components) and low frequency (long periodic components) constituents (Drago and Boxall, 2002). This is one of the main reasons that the WT is more advantageous when used for decomposing signals with non-stationary characteristics, compared to the more conventional spectral analysis, such as the Fourier transform (FT) or windowed Fourier transform (WFT). Fourier Transform uses sine and cosine functions, which do not account for the time information of the signals being analyzed. It therefore cannot provide how information has changed from one time interval to the next (Lau and Weng, 1995). With the WFT, the window used to analyze a time series is fixed, so when there are many different frequencies involved in

the time series, the fixed window picks up more of the high-frequency information but little low-frequency information (Lau and Weng, 1995).

In order to decompose a time series using the WT, the mother wavelet is translated along the signal in a number of steps (using high-pass and low-pass filters). This procedure then produces wavelet coefficients, which measure the correlation of the wavelet to the original signal at a specific scale as a function of time – this is the time-scale representation of the signal, which holds information about the magnitude and location of different events at difference scales (Lindsay et al., 1996; Drago and Boxall, 2002). Different scales are represented by different stretched versions of the mother wavelet.

The WT can be performed either in continuous or discrete modes. Signal reconstructions from the wavelet coefficients are relatively simple to compute when the DWT approach is used – this is done by using the inverse filter function of the wavelet transform (Torrence and Compo, 1998). Signal reconstructions for the CWT, on the other hand, are somewhat problematic because of the redundancy in the time-scale information (Torrence and Compo, 1998). The DWT mode also operates on dyadic scales separating the analyzed signal scale by scale – this is another advantage of using the DWT approach (Lindsay et al., 1996). The signal decomposition using DWT starts out with the smallest scales and continues to larger scales, doubling in size for each round of operation.

The decomposition of a time series  $x_t$  via the WT is accomplished using the following function (Lau and Weng, 1995):

$$\Psi_{a,s}(t) = \frac{1}{\sqrt{s}} \Psi\left(\frac{t-a}{s}\right) \quad (1)$$

where  $s$  (which is greater than zero) represents the scaling factor,  $a$  is the translation factor, and  $\Psi(t)$  is the analyzing wavelet. The wavelet coefficients ( $C$ ) via the CWT for the time series  $x_t$  (with equal time interval,  $dt$ ), are calculated as follows (Lau and Weng, 1995):

$$C(a,s) = \frac{1}{\sqrt{s}} \int \Psi^* \left( \frac{t-a}{s} \right) x(t) dt \quad (2)$$

where  $\Psi^*$  is the complex conjugate number based on the scaling ( $s$ ) and translation ( $a$ ) factors. The wavelet coefficients ( $w$ ) via the discrete wavelet approach for the time series (with dyadic grid arrangement) are calculated as follows (Partal and Küçük, 2006):

$$w(a,s) = \frac{1}{(2)^{\frac{s}{2}}} \sum_{t=0}^{N-1} x_t \Psi \left( \frac{t}{2^s} - a \right). \quad (3)$$

## 2.2. The original Mann–Kendall (MK) trend test

The original MK test is based on Mann (1945) and Kendall (1975). It is a rank correlation test for two sets of observations between the rank order of the recorded values and their ordered values in time. The null hypothesis of the MK test for a dataset ( $X_h$ ,  $h = 1, 2, 3, \dots, n$ ) is that the dataset is independent and identically distributed (Yue et al., 2002). The alternative hypothesis would state that a monotonic

trend is contained in the dataset. The calculation of the MK test statistic, which is also known as Kendall's tau, is as follows (Yue et al., 2002):

$$S_k = \sum_{h=1}^{n-1} \sum_{i=h+1}^n \text{sign}(X_i - X_h) \quad (4)$$

$X_i$  denotes the ordered data values, and  $n$  is the length of observations; the sign test is (Yue et al., 2002):

$$\text{Sign}(X_i - X_h) = \begin{cases} +1 & \text{if } X_i > X_h \\ 0 & \text{if } X_i = X_h \\ -1 & \text{if } X_i < X_h \end{cases} \quad (5)$$

When the number of observations is greater than 10, the Kendall's tau  $S_k$  has a distribution that is approximately normal with zero mean (Hamed and Rao, 1998; Adamowski and Bougadis, 2003). The variance of the statistic  $S_k$  can then be calculated using the following equation (Kendall, 1975; Yue et al., 2002):

$$V(S_k) = \left\{ n(n-1)(2n+5) - \sum_{h=1}^{nh} t_h(h-1)(2h+5) \right\} / 18 \quad (6)$$

$t_h$  represents the number of ties or duplicates of extent  $h$  (the summation in Eq. (6) is used in the presence of tied values in the time series).  $nh$  is the total number of ties in the dataset. When  $n \geq 10$  the standardized test statistic for the Mann–Kendall test can then be calculated using (Yue et al., 2002):

$$Z = \begin{cases} \frac{S_k - 1}{\sqrt{V(S_k)}}, & \text{(if } S_k > 0) \\ 0, & \text{(if } S_k = 0) \\ \frac{S_k + 1}{\sqrt{V(S_k)}}, & \text{(if } S_k < 0) \end{cases} \quad (7)$$

Positive and negative  $Z$  values indicate that the direction of the trend is upward and downward, respectively. The calculated  $Z$  value is compared to the standard normal variate at some level of statistical significance ( $\alpha$ ) (Hamed and Rao, 1998). In a two-sided test, if the calculated  $|Z|$  is greater than  $Z_{\alpha/2}$ , it implies that there is a significant trend (i.e. the null hypothesis is rejected).

## 2.3. Modified Mann–Kendall (MK) trend tests

It is important to check for the presence of serial correlation in the time series being analyzed prior to using the original MK test. It is widely recognized that the original MK trend test should only be applied to test for a trend in a dataset that does not exhibit serial correlation (Hamed and Rao, 1998; Adamowski and Bougadis, 2003; Mohsin and Gough, 2010). If the original MK test is used on a time series that exhibits positive serial correlation, the likelihood of finding trends is enhanced, when in fact, there is no trend; and vice versa (Hirsch and Slack, 1984; Hamed and Rao, 1998). Hamed and Rao (1998) tested a time series with an AR(1) of 0.4 using the original MK test and they were able to demonstrate that the significant positive trend found (at the 5% significance level) was merely due to the effect of autocorrelation in the data.

Modifications to the original MK test have been proposed by Hirsch and Slack (1984) and Hamed and Rao (1998) in order to account for seasonality patterns and autocorrelation factors in the analyzed data, respectively. These modified versions of the MK tests are summarized in the following sections.

### 2.3.1. Modified Mann–Kendall (MK) test by Hirsch and Slack (1984) for data with seasonality patterns and autocorrelation

For a dataset,  $x$ , recorded over  $v$  season and for  $u$  years, with no missing or tied values, its matrix can be written as (Hirsch and Slack, 1984):

$$x = \begin{pmatrix} x_{11} & x_{12} & x_{13} \dots & x_{1v} \\ x_{21} & x_{22} & x_{23} \dots & x_{2v} \\ x_{31} & x_{32} & x_{33} \dots & x_{3v} \\ \dots & \dots & \dots & \dots \\ x_{u1} & x_{u2} & x_{u3} \dots & x_{uv} \end{pmatrix}. \quad (8)$$

The ranks of the data in matrix  $x$  are represented by matrix  $r$  (Hirsch and Slack, 1984):

$$r = \begin{pmatrix} r_{11} & r_{12} & r_{13} \dots & r_{1v} \\ r_{21} & r_{22} & r_{23} \dots & r_{2v} \\ r_{31} & r_{32} & r_{33} \dots & r_{3v} \\ \dots & \dots & \dots & \dots \\ r_{u1} & r_{u2} & r_{u3} \dots & r_{uv} \end{pmatrix}. \quad (9)$$

The seasonal Kendall test statistic, which is asymptotically normal with a mean of zero, is calculated using the sum of the Mann–Kendall test statistic for each season. The variance of the seasonal Kendall test statistic is then calculated by adding the sum of the variance from each season with the estimate covariance of two seasons (which was developed by Dietz and Killeen (1981)). The estimate of covariance of two seasons relies on the Spearman's correlation coefficient for cases that have no ties and no missing values. Hirsch and Slack (1984) demonstrated that by using these consistent estimators for the covariance in order to calculate the variance of the seasonal Kendall test statistic, the assumption of independence in a time series is no longer required. The details of this modified version of the MK test can be found in Hirsch and Slack (1984).

### 2.3.2. Modified Mann–Kendall (MK) test by Hamed and Rao (1998) for significantly autocorrelated data

The Hamed and Rao (1998) modified version of the MK test is intended to address the serial correlation structures in a dataset by looking at their effects on the mean and variance of the original Mann–Kendall test. An empirical approximation for the variance for the MK test was developed, which is considered suitable for autocorrelated data. The calculation of the variance of the MK test statistic is altered by incorporating the effective number of samples required to account for the autocorrelation in the dataset in to the calculation — the autocorrelation between ranks is used instead of between the data values. The details of this modified version of the MK test can be found in Hamed and Rao (1998).

Hamed and Rao (1998) applied their proposed modified version of the MK test on precipitation and streamflow series exhibiting autocorrelation and found that the power of the test is similar when compared to that of the original MK test (for independent data). The accuracy of this modified MK test is much higher than the original MK test for data that exhibit significant autocorrelation. Hamed and Rao (1998) also showed that the empirical significance level is much closer to the nominal significance level when the modified MK test is used in autocorrelated data.

## 3. Data and study sites

Data from a total of five meteorological stations located in southern Ontario and Quebec were used in this study. Harrow, Vineland, Belleville and Peterborough stations are located in Ontario and Val d'Or station is located in Quebec. For the purpose of analyzing trends associated with climate change, Kahya and Kalayci (2004) and Burn and Hag Elnur (2002) recommended that at least 31 and 25 years worth of data, respectively, are used in order to obtain a valid mean statistic. Partal (2010) considered 40 years' worth of data adequate for trend analysis studies. Additionally, Mishra and Singh (2010) considered that up to 3% of missing records are acceptable for trend analysis in meteorological studies. In light of this, the stations selected in this study have at least 40 years of data without any missing values. A number of studies looking at trends in hydroclimatic indices have also used 40 years worth of data or less (e.g. Domroes and El-Tantawi, 2005; Chaouche et al., 2010; Makokha and Shisanya, 2010; Karaburun et al., 2011).

The locations of the stations used in the study are shown in Fig. 1; and the key features of the stations are given in Table 1 — joint stations indicate that records from nearby stations were combined in order to produce longer time series. The details of how data from nearby stations were combined can be found in Mekis and Vincent (2011).

The data used in this study came from the second generation homogenized temperature data of Environment Canada. These homogenized temperature data are specially developed for trend studies in climatic indices. Adjustment procedures on monthly and daily maximum and daily minimum temperature indices were implemented to create the first generation homogenized temperature data. The adjustments were applied in order to account for non-climatic shifts such as station relocations, changes in recording procedures and automation (Vincent and Gullett, 1999). These non-climatic shifts may cause inhomogeneities in the temperature data, which in turn leads to inaccurate trend estimates if the data were to be used for trend analysis (Zhang et al., 2000). In the second generation homogenized sets, the spatial and temporal coverage of temperature data have been improved. Furthermore, additional adjustment procedures were implemented in order to solve the bias caused by the redefinition of the end time of the climatological day, which occurred as of July 1, 1961 (refer to Vincent et al., 2009 for the details of the adjustments). The adjustment procedures in the second generation homogenized datasets involved adjusting the daily minimum temperatures, which are based on hourly data for the period 1967–2006 (40 years) — the adjustment in any one day was between 0.58 and 12.58 °C (Vincent et al., 2009).

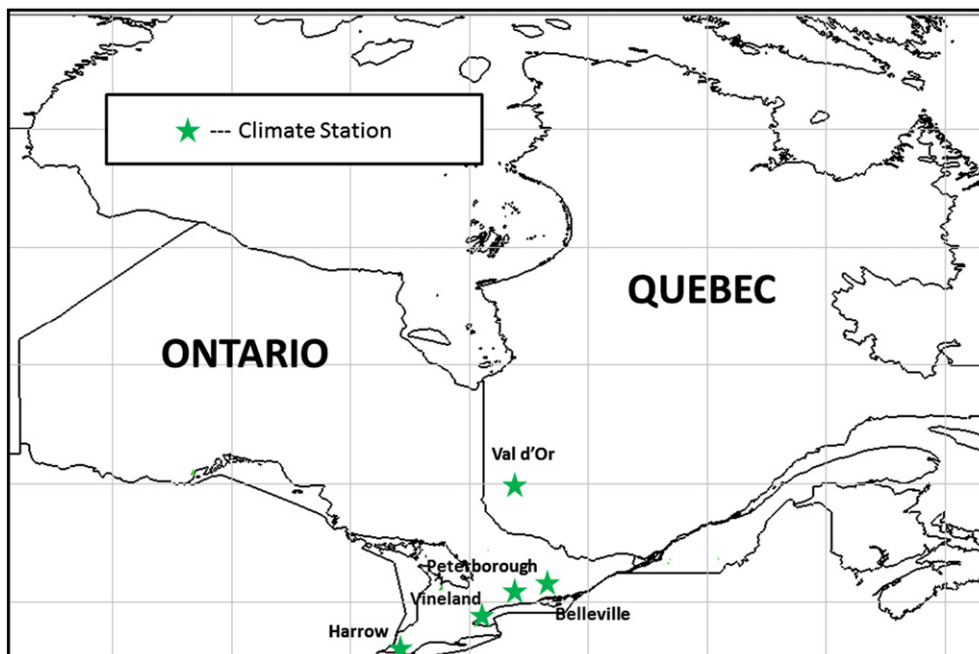


Fig. 1. The map of the weather stations used in this study.

There are four categories of temperature data analyzed in our study: monthly, seasonally-based, seasonal (i.e. winter, spring, summer, and autumn), and annual. The data spanned from 1967 to 2006, with the exception of station Harrow, whose annual and autumn data end in 2005 due to missing observations at the end of 2006.

The monthly data contain observations starting from January 1967 to December 2006 (with the exception of station Harrow whose monthly time series ends in August 2006). Seasonally-based data use the average value from each season every year continuously from winter 1967 to autumn 2006 (with the exception of station Harrow whose seasonally-based data ends in summer 2006): December–February (winter), March–May (spring), June–August (summer), and September–November (autumn). In the seasonal data analysis, each season (i.e. winter, spring, summer, and autumn) was analyzed separately.

Monthly data were analyzed in order to investigate the effects of shorter time scales (e.g. intra-annual and inter-annual periodicities) on the observed temperature trends. Seasonally-based time series were analyzed in order to investigate the effects of the semi-annual and annual seasonality on the temperature trends. Annual and seasonal time series were included in the study in order to investigate events occurring in

longer time scales such as multi-year and decadal events. Additionally, seasonal data were included because several studies found that changes in temperature do not only occur in annual data but also within the different seasons (examples for Canada: Zhang et al., 2000; Vincent et al., 2007). Karaburun et al. (2011) also indicated that an overall positive trend in the mean annual temperature data may not show that trends in some seasons may actually be negative. Therefore, it is important to analyze individual seasons separately.

#### 4. Methodology

The wavelet decomposition was applied to each time series in order to separate their high- and low-frequency components. After the decomposition, the MK trend test was then applied to the different detail components (D), approximation components (A), as well as to the detail components with their respective approximation added. The data analysis in this study was carried out using several procedures, which are summarized as follows:

1. The presence (or lack thereof) of serial correlation was checked for each dataset.
2. The presence (or lack thereof) of seasonality patterns in each dataset was determined using their correlograms.
3. Each time series was decomposed via the DWT into its details (D) and approximation (A) components. The type of mother wavelet, number of decomposition levels, and the type border extension used were determined using the relative error criterion between the MK Z-values of the original data and the approximation component at the last decomposition level (see Section 4.2).
4. The MK trend test and the sequential MK analysis were applied to the original datasets and to the different detail and approximation series produced by the wavelet decomposition.

Table 1  
Key features of the meteorological stations used in this study.

Station name	Province	Station location		Elevation (m)	Joint station
		Latitude (°)	Longitude (°)		
Harrow	ON	42.0	−82.9	182	Yes
Vineland	ON	43.2	−79.4	79	Yes
Belleville	ON	44.2	−77.4	76	No
Peterborough	ON	44.2	−78.4	191	Yes
Val d'Or	QC	48.1	−77.8	337	No

5. The most important periodicities that affect the observed trends were determined by examining the sequential MK graphs and the MK Z-values of the detail (plus approximation) components, and then comparing them to that of the original data.

4.1. Serial correlation and seasonality analyses

The serial correlation test was applied in order to check if a time series exhibited non-random characteristics. If serial correlation exists in a time series, it increases the likelihood to reject the null hypothesis of no trend, when in fact the null hypothesis should be accepted (Yue et al., 2002). This is because the variance of the MK test statistic is underestimated (Hamed and Rao, 1998).

In this study, each time series' correlograms and autocorrelation coefficients (ACFs) at lag-1 were used to determine the presence (or lack thereof) of a significant autocorrelation. Lag-1 ACF is commonly used to determine whether a time series exhibit non-random characteristics (e.g. Partal and Kahya, 2006; Mohsin and Gough, 2010). Lag-1 ACFs were computed using (Yue et al., 2002; Mohsin and Gough, 2010):

$$R = \frac{\left(\frac{1}{n-1}\right) \sum_{t=1}^{n-1} [x_t - \bar{x}_t] [x_{t+1} - \bar{x}_t]}{\left(\frac{1}{n}\right) \sum_{t=1}^n [x_t - \bar{x}_t]^2} \tag{10}$$

$$\frac{\{-1 - 1.645 \sqrt{n-2}\}}{n-1} \leq R \leq \frac{\{-1 + 1.645 \sqrt{n-2}\}}{n-1} \tag{11}$$

R represents the autocorrelation coefficient at lag-1 of the time series  $x_t$ ,  $\bar{x}_t$  represents the mean of the data. If the calculated lag-1 ACF is found to be within the interval defined by Eq. (11), it can be concluded that the time series does not exhibit a significant autocorrelation. On the contrary, if the calculated lag-1 ACF is outside of the interval, it can be said

that the time series exhibits a significant autocorrelation at the 5% significance level.

The correlograms depicting the ACFs of the analyzed time series at different lags were obtained using IBM SPSS Statistics 19. If an ACF value crosses the upper or lower confidence limits, it indicates that the autocorrelation at that specific lag is significant (an example is given in Fig. 2). The correlograms were also used to identify whether a particular time series exhibits some form of seasonality. If repeated oscillating patterns that continued for many lags were observed in a correlogram, it indicates that the analyzed time series exhibited seasonality patterns (as exemplified in Figs. 2 and 3).

4.2. Discrete wavelet transform (DWT) applications on different temperature time series

Time series decomposition via the DWT was computed using the *multilevel one-dimensional wavelet analysis* function in MATLAB. The signal (i.e. time series) is convolved with low-pass and high-pass filters, followed by a dyadic discretization or downsampling procedure, in order to produce the approximation (A) and detail (D) coefficients. The signal is then reconstructed using the *multilevel one-dimensional wavelet reconstruction* function using the same band-pass filters. The original signal is decomposed into scales by powers of 2: the signal is broken down in halves, then in quarters, and it continues onward (Dong et al., 2008). The first decomposition results in detail (D1) and approximation (A1), the next iteration decomposes A1 into detail (D2) and approximation (A2); the process repeats until the desired number of decomposition levels is reached. The lower the level of the detail (D) component, the higher the frequency of information it represents. The lowest frequency information of the data is contained in the approximation (A) component of the last decomposition level. A perfect reconstruction of the original signal can then be achieved by working the calculation

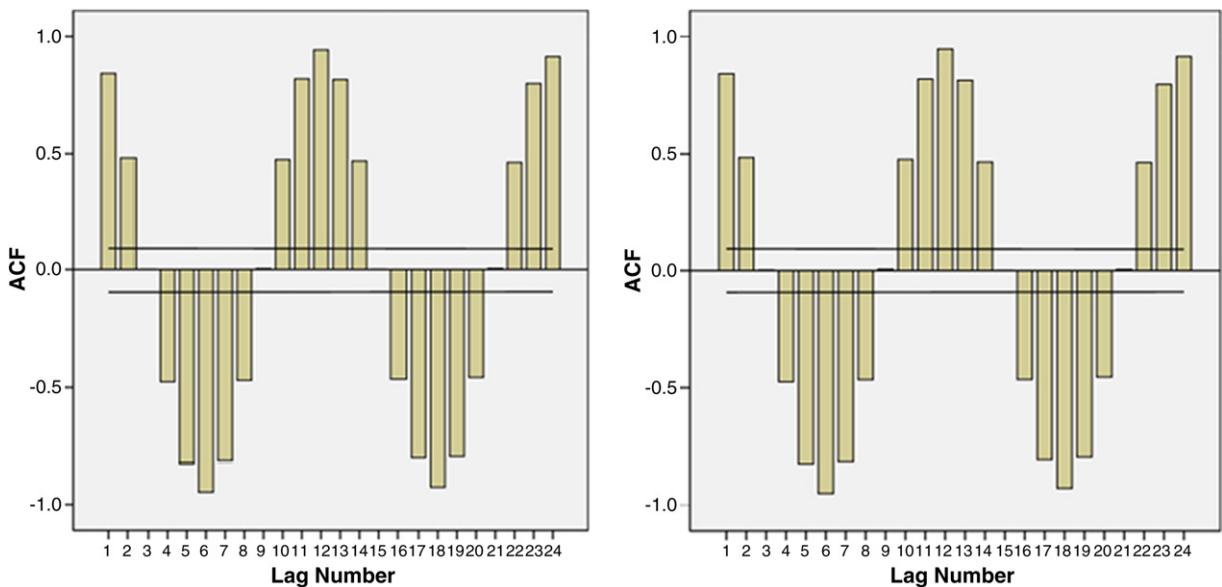
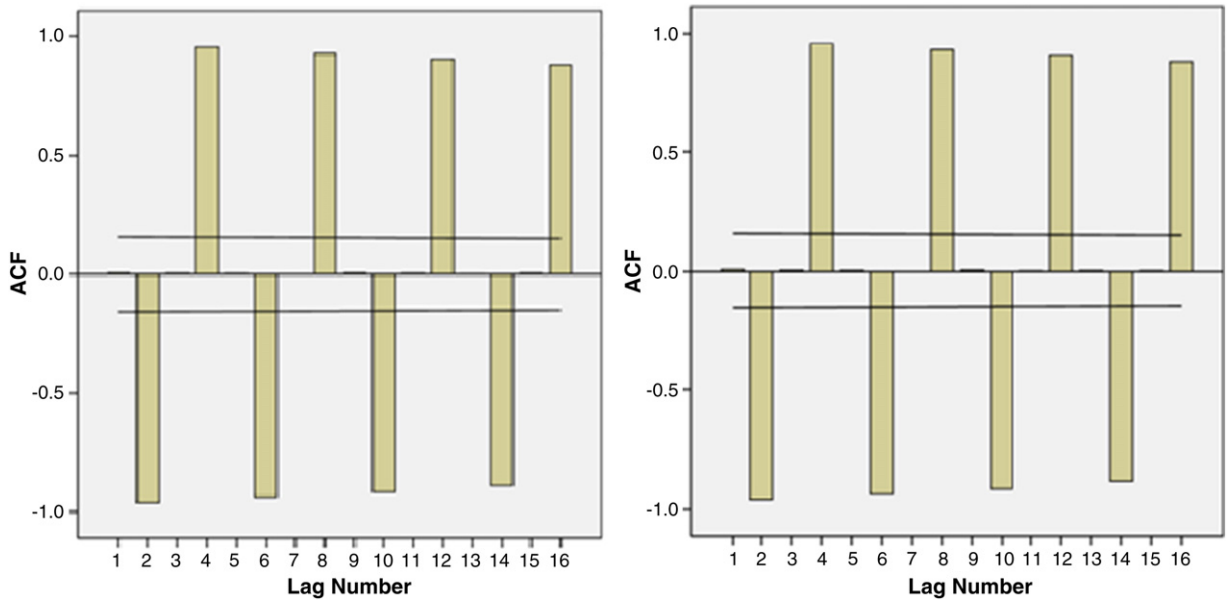


Fig. 2. Examples of the monthly data correlograms: stations Harrow (left) and Vineland (right). High coefficient values at every sixth lag indicate the presence of semi-annual and annual seasonality patterns. The upper and lower confidence limits are shown by the straight lines.



**Fig. 3.** Examples of the seasonally-based data correlograms: stations Harrow (left) and Vineland (right). High coefficient values at every second lag indicate the presence of semi-annual and annual seasonality patterns. The upper and lower confidence limits are shown by the straight lines.

upwards from the approximation (A) component of the last decomposition level.

Daubechies (db) wavelets were used as the mother wavelet in the time series decomposition. The Daubechies (db) wavelets were used in this study because of their ease of use, compact support, and orthogonality (Ma et al., 2003; Vonesch et al., 2007), which implies that the wavelets have non-zero basis functions over a finite interval, and also full scaling and translational orthonormality properties (Popivanov and Miller, 2002; de Artigas et al., 2006). These properties are very important for localizing events when analyzing signals that are characterized by time dependency – this localizing property also implies that wavelets can be adjusted to accommodate both high and low frequencies of the analyzed signals (Wang et al., 1998; Popivanov and Miller, 2002). Furthermore, the compact support provided by Daubechies (db) wavelets has fewer degrees of freedom (associated with the wavelet coefficients), which is ideal for analyzing signals with complex structures (Ma et al., 2003). The scaling function of a Daubechies (db) wavelet also effectively represents polynomials with order up to  $\phi/2-1$ , where  $\phi$  is an even integer (Ma et al., 2003). In order to determine the type of Daubechies (db) wavelet to be used in the time-series decomposition, this present study tried out different wavelets from db1 to db10.

Border extensions were also considered important because when performing the DWT decomposition on signals with finite length, the issue of border distortion effects is introduced. This happens because convolution processes cannot occur outside the ends of signals having limited length as there is no available information outside the ends (Su et al., 2011). Extending the ends of the signal produces several extra coefficients during the decomposition process, which are needed to ensure a perfect signal reconstruction. There are three types of border extensions that are normally used in the DWT: zero padding, periodic extension, and boundary value replication (symmetrization). Zero padding uses zeros outside of the original support of the

mother wavelet, to pad the signal being analyzed; periodic padding recovers the signal beyond the original support by periodic extension; and symmetrization – which is the default mode in MATLAB – assumes that signals outside the original support can be recovered by symmetric boundary replication (de Artigas et al., 2006). The inverse discrete wavelet transform (IDWT) was then run in MATLAB to ensure perfect signal reconstructions.

In this study, two criteria were tried out in order to calculate the number of decomposition levels and to determine the border extension and the type of Daubechies (db) mother wavelet to be used in the DWT procedure. The first criterion involved the use of the mean relative error (MRE) between the approximation (A) time series and original time series. The second criterion used the relative error (RE) between the MK Z-values of the approximation (A) of the last decomposition level and the original data. The lowest MRE and RE values were sought. The MRE was calculated using (Popivanov and Miller, 2002; de Artigas et al., 2006):

$$MRE = 1/n \sum_{j=1}^n \frac{|a_j - x_j|}{|x_j|} \quad (12)$$

where  $x_j$  is the original data value of a signal whose number of records is  $n$ , and  $a_j$  is the approximation value of  $x_j$ . The RE criterion was proposed by Nalley et al. (2012) and calculated using:

$$RE = \frac{|Z_{ap} - Z_{or}|}{|Z_{or}|} \quad (13)$$

$Z_{or}$  represents the MK Z-value of the original time series; and  $Z_{ap}$  is the MK Z-value of the approximation component of the last decomposition level of the DWT.

The following equation was proposed by de Artigas et al. (2006), who conducted a study on monthly geomagnetic activity indices, to calculate the number of decomposition levels:

$$L = \frac{\text{Log}\left(\frac{n}{2v-1}\right)}{\text{Log}(2)} \quad (14)$$

where  $v$  represents the number of vanishing moments of a Daubechies (db) wavelet,  $n$  is the number of records in a monthly-based time series, and  $L$  is the maximum decomposition levels. In MATLAB, the number of vanishing moments for a Daubechies (db) wavelet is half of the length of its starting filter. For example, if one is using the db3 mother wavelet in MATLAB, it implies that the wavelet is Daubechies3, which has a 6-point filter length. It should also be noted that if the number of data points in a time series is not exactly in a dyadic format (as is the case in this study), the DWT computation in MATLAB is performed using the next dyadic arrangement. For example, in our study there were 480 data points in monthly datasets. The value of  $n$  in Eq. (14) would be represented by  $2^9 = 512$  (which is the next dyadic format from 480). Therefore, the number of  $n$  used in the DWT procedure would be 512. If, for example, the db3 wavelet is used on the monthly data, the number of decomposition levels,  $L$ , would be 6.68 (seven levels would then be used). Similarly, for the seasonally-based time series (having 160 data points), the computation of the DWT in MATLAB would use 256 ( $2^8$ ) as  $n$ . If db3 was used in Eq. (14) for the seasonally-based data, the calculated  $L$  would be 5.68 (six levels would then be used).

The use of the newly proposed *RE* criterion by Nalley et al. (2012) illustrated that using the *RE* was more precise in determining the most appropriate type of Daubechies (db) mother wavelet and border extension, and the number of decomposition levels. This provides a justification to use this criterion for the DWT computation in our study. When the *MRE* criterion was used to determine the number of decomposition levels (using different db types and border extensions), the differences in the *MRE* between different decomposition levels were not noticeable. For example, for station Vineland's annual data, the *MRE* for four decomposition levels using different Daubechies (db) wavelets ranged from: 0.06 to 0.07, 0.055 to 0.059, and 0.11 to 0.22 using periodic extension, symmetrization, and zero padding, respectively. The *MRE* for five decomposition levels for the same station ranged from: 0.06 to 0.08, 0.06 to 0.07, and 0.19 to 0.24 using periodic extension, symmetrization, and Zero padding, respectively. On the contrary, when the *RE* criterion was used, noticeable differences were observed. For example, for Vineland's annual data, the relative errors obtained from using four decomposition levels were: 0.01–1.58, 1.00–3.40, and 0.03–1.84 using periodic extension, symmetrization, and zero padding, respectively. For the same data, the relative errors obtained from using five decomposition levels were: 0.02–2.16, 0.58–7.66, and 0.04–2.60 using periodic extension, symmetrization, and zero padding, respectively. Therefore, for Vineland's annual data, four decomposition levels were used (the lowest *RE* of 0.01 was obtained from using db6 wavelet). This is an example of how the number of decomposition levels was determined on a case-by-case basis in this

study. The noticeable differences in the *RE* were not only seen for Vineland station, but also for all the other stations.

In our study, we observed that in most cases, using db wavelets or border extensions, other than the ones determined using the *RE* criterion, led to a different number of decomposition levels. Generally the number of decomposition levels was different by one (the analysis is not presented here). Even so, the most dominant periodicities (based on the MK Z-values of the detail components and their sequential MK graphs) may not be the same as those resulting from when the *RE* criterion was used. In addition to that, if data decomposition is done using Daubechies (db) wavelets and border extensions other than the ones determined using the *RE* criterion, the sequential MK graphs of the detail components (even for those whose MK Z-values are closest to that of the original data) are out of harmony compared to the sequential MK of the original data.

#### 4.3. The Mann–Kendall (MK) trend test

The MK test statistic  $S$  and the variance were calculated (see Eqs. (4) and (6), respectively) for each dataset in order to obtain the standard normal value,  $Z$  score (see Eq. (7)). In the data analysis of this study, the significant level used was  $\alpha = 5\%$  (or 95% confidence level) for a two-sided probability. The absolute value of this  $Z$ -score was then compared to the critical value of this two-tailed  $Z$ -value (area under the normal curve) of  $\alpha/2$ . The  $Z$  values in a two-tailed test for  $\alpha = 5\%$  are  $\pm 1.96$ . If the calculated MK  $Z$ -score is outside the range of  $-1.96$  and  $+1.96$ , the trends are statistically significant. The MK test tests the null hypothesis of no trend (independent observations and ordered randomly) against the alternative hypothesis of positive or negative monotonic trends over time that are present in the dataset being analyzed (Hirsch and Slack, 1984; Mohsin and Gough, 2010; Karaburun et al., 2011).

##### 4.3.1. Applications of the original and modified versions of the Mann–Kendall (MK) trend test

The modified MK test by Hirsch and Slack (1984) was used on time series that exhibited seasonality patterns. The modified MK test by Hamed and Rao (1998) was used on time series that exhibited only significant autocorrelations at lag-1. The original MK test was applied to time series that exhibited neither significant autocorrelations at lag-1 nor seasonality patterns.

##### 4.3.2. Sequential Mann–Kendall (MK) analysis

The sequential MK test was used in order to examine the progressive trend lines in each time series from the beginning to the end of the study period. This is useful because positive and negative trends, which may or may not be significant, can be observed in the sequential MK graphs (Makokha and Shisanya, 2010). Additionally, with sequential MK analysis, we could also observe if a series of significant positive and negative trends may cancel each other out and thus, produce an MK  $Z$ -value that is not significant at the end of the study period. The sequential MK analysis in this study was also used to determine the periodic modes that are considered the most influential in affecting the temperature trends over the study area.

The sequential MK values were calculated using the appropriate MK test (i.e. the original or the modified versions) for each dataset, from the start to the end of the study period.

The sequential MK values were then graphed. In the sequential MK graph, the upper and lower lines correspond to the confidence limits of the standard normal Z values at  $\alpha = 5\%$ . The upper and lower confidence limits therefore, correspond to  $+1.96$  and  $-1.96$ , respectively. When the sequential MK value crosses either one of the confidence limit lines it indicates a significant trend at the 5%-significance level – crossing the upper line implies a significant positive trend, whereas crossing the lower line implies a significant negative trend.

It is important to recall that the standard normal Z-score can be used in the MK test only when the number of observations in a dataset is more than 10. With this in mind, the accuracy of the first 10 sequential MK values (i.e. up to year 1976) in the sequential MK graphs may be overlooked.

## 5. Results and discussions

### 5.1. Preliminary data analysis

#### 5.1.1. Serial correlation and seasonality factors

All the monthly data showed significant lag-1 autocorrelation coefficients (Table 2). For all other data categories, significant lag-1 autocorrelation coefficients were only observed for station Vineland's annual data ( $R = 0.35$ ) (Table 2). It is commonly expected that a monthly time series would have a stronger autocorrelation compared to its annual counterparts (Hirsch and Slack, 1984). The correlograms of all the monthly data also showed strong seasonality patterns as there are repeated patterns of cycles. Semi-annual and annual seasonality patterns are strongly apparent in all the monthly data as there are high coefficients at every 6th lag (Fig. 2). This is again confirmed by the correlograms of the seasonally-based data, where the autocorrelation functions are much higher at every 2nd lag (Fig. 3). The 2nd and 4th lags in the seasonally-based data correspond to 6 and 12 month cycles, respectively.

#### 5.1.2. The Mann–Kendall (MK) test on original data

Due to the presence of seasonality patterns in the monthly and seasonally-based data, the modified version of the MK test by Hirsch and Slack (1984) was used on these data sets. The original MK test was used on the seasonal and annual datasets that showed an absence of serial correlations. The modified MK version by Hamed and Rao (1998) was used on the annual data for Vineland station because it is the only dataset that exhibits a significant lag-1 autocorrelation.

As shown in Table 3, all of the trend values show positive signs, which indicate that all temperature indices analyzed in this study have positive trends. For the monthly, seasonally-

**Table 3**

Mann–Kendall Z-values of the original time series for the different temperature data types.

	Harrow	Vineland	Belleville	Peterborough	Val d'Or
Monthly data	3.25 <sup>a</sup>	3.39 <sup>a</sup>	3.33 <sup>a</sup>	2.45 <sup>a</sup>	2.80 <sup>a</sup>
Seasonally-based data	3.09 <sup>a</sup>	3.25 <sup>a</sup>	3.26 <sup>a</sup>	2.48 <sup>a</sup>	2.57 <sup>a</sup>
Annual data	2.88 <sup>a</sup>	3.15 <sup>a</sup>	3.58 <sup>a</sup>	2.49 <sup>a</sup>	2.18 <sup>a</sup>
Winter data	1.97 <sup>a</sup>	1.97 <sup>a</sup>	2.60 <sup>a</sup>	2.37 <sup>a</sup>	1.80
Spring data	1.67	2.15 <sup>a</sup>	1.59	1.09	1.03
Summer data	2.87 <sup>a</sup>	2.81 <sup>a</sup>	2.59 <sup>a</sup>	1.87	1.98 <sup>a</sup>
Autumn data	1.21	1.73	1.69	0.91	1.38

<sup>a</sup> Indicates a significant trend value at  $\alpha = 5\%$ .

based, and annual data analysis, all stations are experiencing statistically significant positive trends (at the 5%-level). For the seasonal data, most stations are experiencing significant positive trends for the winter season (except for station Val d'Or) and for the summer season (except for station Peterborough) – it should be noted however, that the MK Z-value of Val d'Or winter and Peterborough summer are  $+1.80$  and  $+1.87$ , respectively, which are just slightly below  $+1.96$ . Only station Vineland showed a significant trend value for the spring season; and there was no station with significant trend values for autumn.

#### 5.1.3. The number of decomposition levels for the different time series

The number of decomposition levels for each time series (Tables 4–10) was determined using the MK Z-value *RE* criterion. As explained in Section 4.2, the lowest relative error of the MK Z-value produced from using the combination of a specific db wavelet and a border extension was sought. As a result, different number of decomposition levels for the same temperature data category may be observed.

Since data decomposition was achieved using the DWT approach, the scales are arranged in a dyadic format (integer powers of two) from the lowest scale. Therefore, D1 represents the 2-unit periodic component, D2 represents the 4-unit periodic component, D3 represents the 8-unit periodic component, and so on. An example of time series decomposition via the DWT is given in Fig. 4. It should be noted that the MK Z-values discussed in the Results and discussions section are of the detail components (D) with their respective approximation component (A) added. The approximation (A) used was the approximation from the last decomposition level. Since the approximation components are representative of the low-frequency component (including trends) (Craigmile et al.,

**Table 2**

Lag-1 autocorrelation functions (ACFs) of the different temperature data types.

	Harrow	Vineland	Belleville	Peterborough	Val d'Or
Monthly data	0.84 <sup>a</sup> (S)				
Seasonally-based data	0.004 (S)	0.008 (S)	0.006 (S)	0.003 (S)	0.001 (S)
Winter data	0.14	0.12	0.19	0.05	−0.10
Spring data	0.05	0.14	0.07	−0.01	−0.02
Summer data	0.03	0.03	−0.06	0.01	−0.10
Autumn data	−0.05	0.12	0.09	0.02	−0.04
Annual data	0.29	0.35 <sup>a</sup>	0.28	0.12	−0.004

(S) indicates the presence of seasonality.

<sup>a</sup> Indicates a significant trend value at  $\alpha = 5\%$ .

**Table 4**

Mann–Kendall Z-values of the monthly temperature series: original data, details components, approximations, and a set of combinations of the details and their respective approximations. The most effective periodic components for trends are indicated in bold format.

	Harrow	Vineleand	Belleville	Peterborough	Val d'Or
Original	3.25 <sup>a</sup>	3.39 <sup>a</sup>	3.33 <sup>a</sup>	2.45 <sup>a</sup>	Original: 2.80 <sup>a</sup>
D1	−0.37	−0.36	0.31	0.00	D1: 0.75
D2	1.49	0.90	0.53	0.71	D2: −0.02
D3	−0.35	−0.67	−0.48	−0.50	D3: 0.41
D4	0.03	0.43	0.46	0.52	D4: 0.04
D5	−0.38	0.59	0.63	0.68	D5: 0.16
D6	1.06	2.03 <sup>a</sup>	1.45	1.63	A5: 2.83 <sup>a</sup>
A6	3.32 <sup>a</sup>	3.55 <sup>a</sup>	3.24 <sup>a</sup>	2.43 <sup>a</sup>	D1 + A5: <b>3.20<sup>a</sup></b>
D1 + A6	<b>3.30<sup>a</sup></b>	<b>3.53<sup>a</sup></b>	<b>3.63<sup>a</sup></b>	<b>2.56<sup>a</sup></b>	D2 + A5: <b>3.27<sup>a</sup></b>
D2 + A6	<b>3.15<sup>a</sup></b>	3.91 <sup>a</sup>	<b>3.62<sup>a</sup></b>	<b>2.55<sup>a</sup></b>	D3 + A5: 2.18 <sup>a</sup>
D3 + A6	1.30	1.68	1.69	0.73	D4 + A5: 1.43
D4 + A6	1.17	1.74	1.57	1.15	D5 + A5: 2.10 <sup>a</sup>
D5 + A6	1.56	2.59 <sup>a</sup>	2.40 <sup>a</sup>	1.65	
D6 + A6	3.63 <sup>a</sup>	4.19 <sup>a</sup>	4.19 <sup>a</sup>	3.71 <sup>a</sup>	

<sup>a</sup> Indicates a significant trend value at  $\alpha = 5\%$ .

2004; Kallache et al., 2005), it makes sense to add them to their detail components prior to testing their trends.

**5.1.4. Determining the most dominant periodic components that affect temperature trends**

Since the main goal of this study was to determine the dominant periodic mode(s) for trend using the DWT approach, it is necessary to select the detail component(s) that best represent the trend in the analyzed data. The coefficients produced from the DWT decomposition are intermediate coefficients and thus, they need to be re-adjusted to the entire signal to determine the contribution of each frequency band to the original signal (Dong et al., 2008). The identity of the signal is contained in the approximation component (Partal, 2010). Therefore, prior to testing the trend of the detail

components, the approximation component should be added to them first – this study used the approximation component of the last decomposition level because it represents the lowest-frequency component of the signal. After doing so, the most dominant periodic components that affect the temperature trends over the study area were determined. Measuring the energy of the components resulting from the DWT decomposition has been used as a way to assess the contribution of certain wavebands in a dataset (examples are seen in Dong et al., 2008; Partal, 2010). In this study, the dominant periodic components for trends were determined in two steps. First, the MK Z-values of each detail component (with its approximation added) were compared to the MK Z-value of their respective original data. Second, the sequential MK values of each detail component (with its approximation added) were graphed along with the sequential MK values of the original data. The periodic component(s) considered the most dominant in affecting the temperature trends are the ones whose MK Z-values were closest to that of the original data and whose sequential MK graphs were the most harmonious with the sequential MK of the original data.

We also tested a number of combinations of detail components with approximation series (e.g. D1 + D2 + A) but the results produced were not conclusive (based on the observations of the MK Z-values and the sequential MK graphs). For example, station Harrow's spring temperature data has an MK Z-value of +1.67; based on the nearest MK Z-value and the sequential MK graphs (see Fig. 10), the D3 component (plus A5) is considered the most dominant periodicity for trend in mean spring temperature data (see Section 5.6 for more detail). When we combine different detail components (with approximation), even when the D3 component is part of the combination set, it does not always produce MK Z-values that are close to the MK Z-value of the original data nor does it produce good sequential MK graphs. For example, D1 + D3 + A5 only gives an MK Z-value of +0.62; D2 + D3 + A5 had an MK Z-value of only +0.57. However, D2 + D5 + A5 produced a relatively close MK Z-value of +1.48, which is close to the MK Z-value of the original data (+1.67), although neither D2 nor D5 was considered important for trends. Therefore, in this study we only chose to include

**Table 5**

Mann–Kendall Z-values of the seasonally-based temperature series: original data, details components, approximations, and a set of combinations of the details and their respective approximations. The most effective periodic components for trends are indicated in bold format.

Harrow	Vineland	Belleville	Peterborough	Val d'or	
Original	3.09 <sup>a</sup>	Original	3.25 <sup>a</sup>	Original	2.57 <sup>a</sup>
D1	0.50	D1	−0.26	D1	0.17
D2	0.19	D2	0.31	D2	0.10
D3	−0.29	D3	0.25	D3	0.50
D4	0.08	D4	0.51	D4	0.53
D5	0.40	D5	−0.27	D5	0.50
D6	1.95	D6	2.01 <sup>a</sup>	D6	0.53
A6	2.69 <sup>a</sup>	A6	3.11 <sup>a</sup>	A6	2.58 <sup>a</sup>
D1 + A6	4.14 <sup>a</sup>	D1 + A6	4.06 <sup>a</sup>	D1 + A6	2.97 <sup>a</sup>
D2 + A6	<b>2.99<sup>a</sup></b>	D2 + A6	<b>3.16<sup>a</sup></b>	D2 + A6	2.96 <sup>a</sup>
D3 + A6	2.90 <sup>a</sup>	D3 + A6	<b>3.36<sup>a</sup></b>	D3 + A6	<b>2.46<sup>a</sup></b>
D4 + A6	<b>3.14<sup>a</sup></b>	D4 + A6	3.70 <sup>a</sup>	D4 + A6	<b>2.55<sup>a</sup></b>
D5 + A6	3.88 <sup>a</sup>	D5 + A6	3.02 <sup>a</sup>	D5 + A6	
D6 + A6	4.39 <sup>a</sup>	D6 + A6	4.97 <sup>a</sup>	D6 + A6	

<sup>a</sup> Indicates a significant trend value at  $\alpha = 5\%$ .

**Table 6**

Mann–Kendall Z-values of the annual temperature series: original data, details components, approximations, and a set of combinations of the details and their respective approximations. The most effective periodic components for trends are indicated in bold format.

Harrow		Vineland		Belleville		Peterborough		Val d'Or	
Original	2.88 <sup>a</sup>	Original	3.15 <sup>a</sup>	Original	3.58 <sup>a</sup>	Original	2.49 <sup>a</sup>	Original	2.18 <sup>a</sup>
D1	−0.15	D1	0.55	D1	0.36	D1	0.22	D1	−0.01
D2	0.31	D2	0.59	D2	0.48	D2	0.80	D2	1.04
D3	0.51	D3	1.25	D3	0.69	D3	0.52	D3	−0.13
D4	0.68	D4	2.92 <sup>a</sup>	D4	3.23 <sup>a</sup>	D4	0.85	D4	1.78
D5	3.70 <sup>a</sup>	A4	3.11 <sup>a</sup>	D5	3.32 <sup>a</sup>	D5	2.37 <sup>a</sup>	D5	2.50 <sup>a</sup>
A5	2.85 <sup>a</sup>	D1 + A4	2.37 <sup>a</sup>	A5	3.72 <sup>a</sup>	A5	2.37 <sup>a</sup>	A5	2.37 <sup>a</sup>
D1 + A5	1.62	D2 + A4	2.27 <sup>a</sup>	D1 + A5	1.29	D1 + A5	0.66	D1 + A5	0.17
D2 + A5	1.98 <sup>a</sup>	D3 + A4	<b>2.90<sup>a</sup></b>	D2 + A5	2.02 <sup>a</sup>	D2 + A5	2.78 <sup>a</sup>	D2 + A5	1.32
D3 + A5	<b>2.71<sup>a</sup></b>	D4 + A4	4.93 <sup>a</sup>	D3 + A5	1.92	D3 + A5	1.41	D3 + A5	0.41
D4 + A5	3.80 <sup>a</sup>			D4 + A5	4.42 <sup>a</sup>	D4 + A5	<b>2.16<sup>a</sup></b>	D4 + A5	<b>2.25<sup>a</sup></b>
D5 + A5	4.94 <sup>a</sup>			D5 + A5	<b>3.23<sup>a</sup></b>	D5 + A5	5.28 <sup>a</sup>	D5 + A5	3.88 <sup>a</sup>

<sup>a</sup> Indicates a significant trend value at  $\alpha = 5\%$ .

**Table 7**

Mann–Kendall Z-values of the winter temperature series: original data, details components, approximations, and a set of combinations of the details and their respective approximations. The most effective periodic components for trends are indicated in bold format.

Harrow		Vineland		Belleville		Peterborough		Val d'Or	
Original	1.97 <sup>a</sup>	Original	1.97 <sup>a</sup>	Original	2.60 <sup>a</sup>	Original	2.37 <sup>a</sup>	Original	1.80
D1	−0.10	D1	0.06	D1	0.24	D1	0.01	D1	0.22
D2	0.29	D2	−0.13	D2	0.41	D2	0.15	D2	−0.06
D3	−0.20	D3	0.90	D3	0.06	D3	0.38	D3	−0.38
A3	2.09 <sup>a</sup>	D4	0.41	D4	2.69 <sup>a</sup>	D4	0.83	D4	0.85
D1 + A3	<b>1.88<sup>a</sup></b>	D5	2.37 <sup>a</sup>	D5	3.95 <sup>a</sup>	D5	2.34 <sup>a</sup>	D5	2.39 <sup>a</sup>
D2 + A3	2.69 <sup>a</sup>	A5	2.37 <sup>a</sup>	A5	2.74 <sup>a</sup>	A5	2.37 <sup>a</sup>	A5	2.37 <sup>a</sup>
D3 + A3	<b>2.23<sup>a</sup></b>	D1 + A5	1.08	D1 + A5	1.08	D1 + A5	1.13	D1 + A5	0.52
		D2 + A5	1.11	D2 + A5	1.55	D2 + A5	1.34	D2 + A5	0.80
		D3 + A5	<b>1.41</b>	D3 + A5	<b>1.64</b>	D3 + A5	1.60	D3 + A5	0.71
		D4 + A5	<b>1.76</b>	D4 + A5	5.04 <sup>a</sup>	D4 + A5	<b>2.39<sup>a</sup></b>	D4 + A5	<b>2.27<sup>a</sup></b>
		D5 + A5	5.28	D5 + A5	4.91 <sup>a</sup>	D5 + A5	5.21 <sup>a</sup>	D5 + A5	5.28 <sup>a</sup>

<sup>a</sup> Indicates a significant trend value at  $\alpha = 5\%$ .

analysis on individual detail components (with their respective approximation components added).

## 5.2. Monthly temperature data analysis

As shown in Table 4, all stations are experiencing significant positive trends. The results of the MK test showed that none of the individual detail components showed significant MK Z-values, except for the D6 component of

station Vineland ( $Z = +2.03$ ) (Table 4). After the addition of the approximation components to their respective details, it is observed that most of the trend values became significant ( $\alpha = 5\%$ ). By examining the sequential MK graphs, and by comparing the MK Z-values of the detail components and the original data, it is found that the periodic components that are effective for trends are relatively similar for all stations. Fig. 5 is an example illustrating how the most dominant periodic component(s) were chosen. Although graphically as

**Table 8**

Mann–Kendall Z-values of the spring temperature series: original data, details components, approximations, and a set of combinations of the details and their respective approximations. The most effective periodic components for trends are indicated in bold format.

Harrow		Vineland		Belleville		Peterborough		Val d'Or	
Original	1.67	Original	2.15 <sup>a</sup>	Original	1.59	Original	1.09	Original	1.03
D1	0.69	D1	0.22	D1	0.83	D1	0.10	D1	0.48
D2	−0.08	D2	0.43	D2	−0.10	D2	0.08	D2	1.11
D3	0.78	D3	1.13	D3	−0.15	D3	0.41	D3	−0.85
D4	7.38 <sup>a</sup>	A3	2.19 <sup>a</sup>	D4	3.58 <sup>a</sup>	A3	1.25	D4	1.97
D5	6.47 <sup>a</sup>	D1 + A3	2.53 <sup>a</sup>	D5	0.24	D1 + A3	0.55	A4	0.92
A5	1.67	D2 + A3	<b>1.99<sup>a</sup></b>	A5	1.67	D2 + A3	0.31	D1 + A4	<b>0.52</b>
D1 + A5	0.73	D3 + A3	3.25 <sup>a</sup>	D1 + A5	<b>0.92</b>	D3 + A3	<b>0.71</b>	D2 + A4	1.88
D2 + A5	0.15			D2 + A5	0.36			D3 + A4	0.00
D3 + A5	<b>0.87</b>			D3 + A5	0.08			D4 + A4	2.69
D4 + A5	7.10 <sup>a</sup>			D4 + A5	3.97 <sup>a</sup>				
D5 + A5	6.05 <sup>a</sup>			D5 + A5	0.80				

<sup>a</sup> Indicates a significant trend value at  $\alpha = 5\%$ .

**Table 9**

Mann–Kendall Z-values of the summer temperature series: original data, details components, approximations, and a set of combinations of the details and their respective approximations. The most effective periodic components for trends are indicated in bold format.

Harrow		Vineland		Belleville		Peterborough		Val d'Or	
Original	2.87 <sup>a</sup>	Original	2.81 <sup>a</sup>	Original	2.59 <sup>a</sup>	Original	1.87	Original	1.98 <sup>a</sup>
D1	0.66	D1	0.85	D1	−0.29	D1	0.78	D1	−0.50
D2	0.55	D2	0.45	D2	0.59	D2	−0.24	D2	0.38
D3	2.23 <sup>a</sup>	D3	2.53 <sup>a</sup>	D3	1.39	D3	1.69	D3	1.15
D4	2.25 <sup>a</sup>	D4	−0.38	D4	5.35 <sup>a</sup>	D4	−0.78	D4	4.53 <sup>a</sup>
D5	3.62 <sup>a</sup>	D5	3.32 <sup>a</sup>	A4	2.35 <sup>a</sup>	A4	1.90	A4	1.85
A5	2.74 <sup>a</sup>	A5	2.74 <sup>a</sup>	D1 + A4	0.48	D1 + A4	1.39	D1 + A4	−0.08
D1 + A5	1.50	D1 + A5	1.53	D2 + A4	1.67	D2 + A4	0.57	D2 + A4	0.92
D2 + A5	<b>1.92</b>	D2 + A5	1.62	D3 + A4	<b>2.25<sup>a</sup></b>	D3 + A4	2.57 <sup>a</sup>	D3 + A4	<b>2.09<sup>a</sup></b>
D3 + A5	<b>3.97<sup>a</sup></b>	D3 + A5	4.09 <sup>a</sup>	D4 + A4	5.23 <sup>a</sup>	D4 + A4	<b>1.74</b>	D4 + A4	2.88 <sup>a</sup>
D4 + A5	4.70 <sup>a</sup>	D4 + A5	<b>3.41<sup>a</sup></b>						
D5 + A5	5.00 <sup>a</sup>	D5 + A5	4.58 <sup>a</sup>						

<sup>a</sup> Indicates a significant trend value at  $\alpha = 5\%$ .

shown in Fig. 5, all detail components show harmonious trend lines, details that have the closest MK Z-values to that of the original data are D1 and D2. The 2-month and 4-month periodic components are the most dominant components for trends in the monthly temperature for stations Harrow, Belleville, Peterborough, and Val d'Or; station Vineland's most dominant component for trends is the 2-month periodicity (Table 4).

As shown in Table 4, the trends for the monthly data in all stations seem to be affected by high-frequency components ranging from 2 to 4 months. Since the data are based on daily measurements, there could be many daily (high-frequency) variations that contribute to the trends in these higher resolution data. Examples of these daily variations are: variation in solar radiation (which can be associated with seasonality), cloud cover, albedo, air moisture content, soil heat capacity, and atmospheric wind movements that can have significant effects on the diurnal temperature (Gough, 2008). Gough (2008) also emphasized that in mid-latitude regions, mid-latitude cyclones may produce temperature clusters whose effects may last for a month. These daily variations may be very strong, and thus, conceal the effects of low-frequency periodicities (i.e. the higher detail components of the DWT).

Although none of the most dominant periodic components for any of the stations are between 6 and 12 months, it is still worthwhile to investigate their seasonally-based data, in order to investigate whether the semi-annual and annual

seasonality may be contributing to the observed warming trends in temperature over the study area.

### 5.3. Seasonally-based temperature data analysis

In this section, particular attention is given to the D1 and D2 detail components because they represent the 6-month and 12-month periodicities, which are assumed to be associated with the seasonality factor observed in the monthly and seasonally-based data. As shown in Table 5, the D2 component is the most frequently observed as the most dominant periodic component affecting trends – except for Val d'Or, all stations have D2 as one of the most dominant periodic components. Fig. 6 illustrates the use of the sequential MK analysis in determining the most harmonious detail component (with the approximation added) for the seasonally-based temperature data. As can be seen in Table 5 and Fig. 6, the yearly fluctuations, which are represented by the D2 component, are contributing in affecting the warming trends in temperature over the study area.

### 5.4. Annual temperature data analysis

Analysis on Canada's annual mean temperature has shown that warming trends are apparent nation-wide. Zhang et al. (2000) reported an increase of 0.5–1.5 °C over the 20th century. Vincent et al. (2007) found that the annual mean temperature in Canada increased by 1.2 °C over the period

**Table 10**

Mann–Kendall Z-values of the autumn temperature series: original data, details components, approximations, and a set of combinations of the details and their respective approximations. The most effective periodic components for trends are indicated in bold format.

Harrow		Vineland		Belleville		Peterborough		Val d'Or	
Original	1.21	Original	1.73	Original	1.69	Original	0.91	Original	1.38
D1	0.15	D1	0.43	D1	0.03	D1	−0.03	D1	−0.03
D2	−0.05	D2	0.76	D2	0.01	D2	0.27	D2	−0.08
D3	−0.07	D3	−1.50	D3	0.48	D3	−0.15	D3	0.18
D4	0.8	A3	1.88	D4	0.66	D4	−0.27	A3	1.51
A4	1.16	D1 + A3	2.16 <sup>a</sup>	A4	1.88	A4	0.85	D1 + A3	<b>1.53</b>
D1 + A4	1.81	D2 + A3	2.06 <sup>a</sup>	D1 + A4	<b>1.48</b>	D1 + A4	1.11	D2 + A3	1.72
D2 + A4	<b>1.31</b>	D3 + A3	<b>1.76</b>	D2 + A4	1.90	D2 + A4	<b>1.01</b>	D3 + A3	1.68
D3 + A4	2.69 <sup>a</sup>			D3 + A4	1.90	D3 + A4	0.76		
D4 + A4	1.86			D4 + A4	2.46 <sup>a</sup>	D4 + A4	−0.48		

<sup>a</sup> Indicates a significant trend value at  $\alpha = 5\%$ .

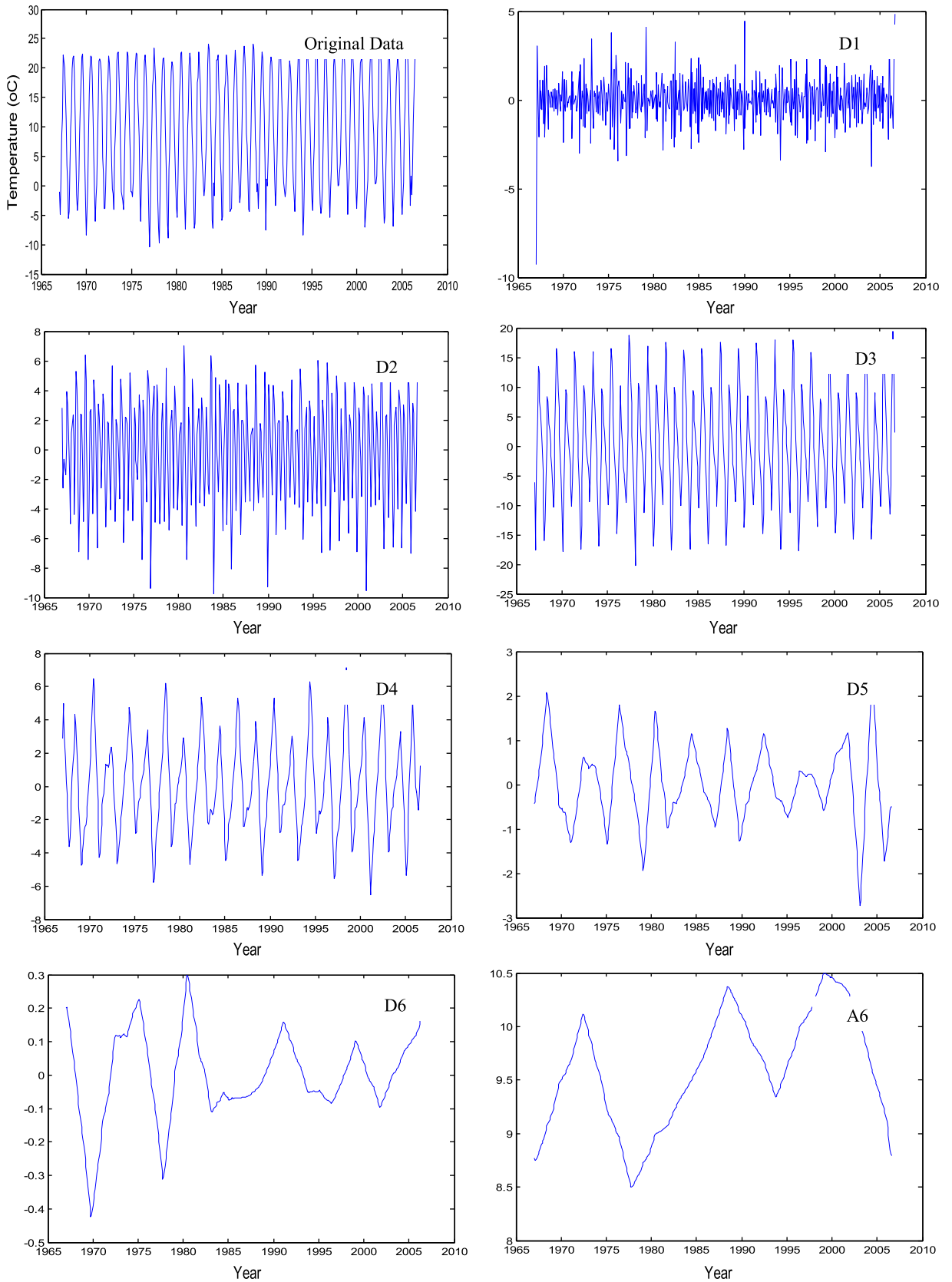
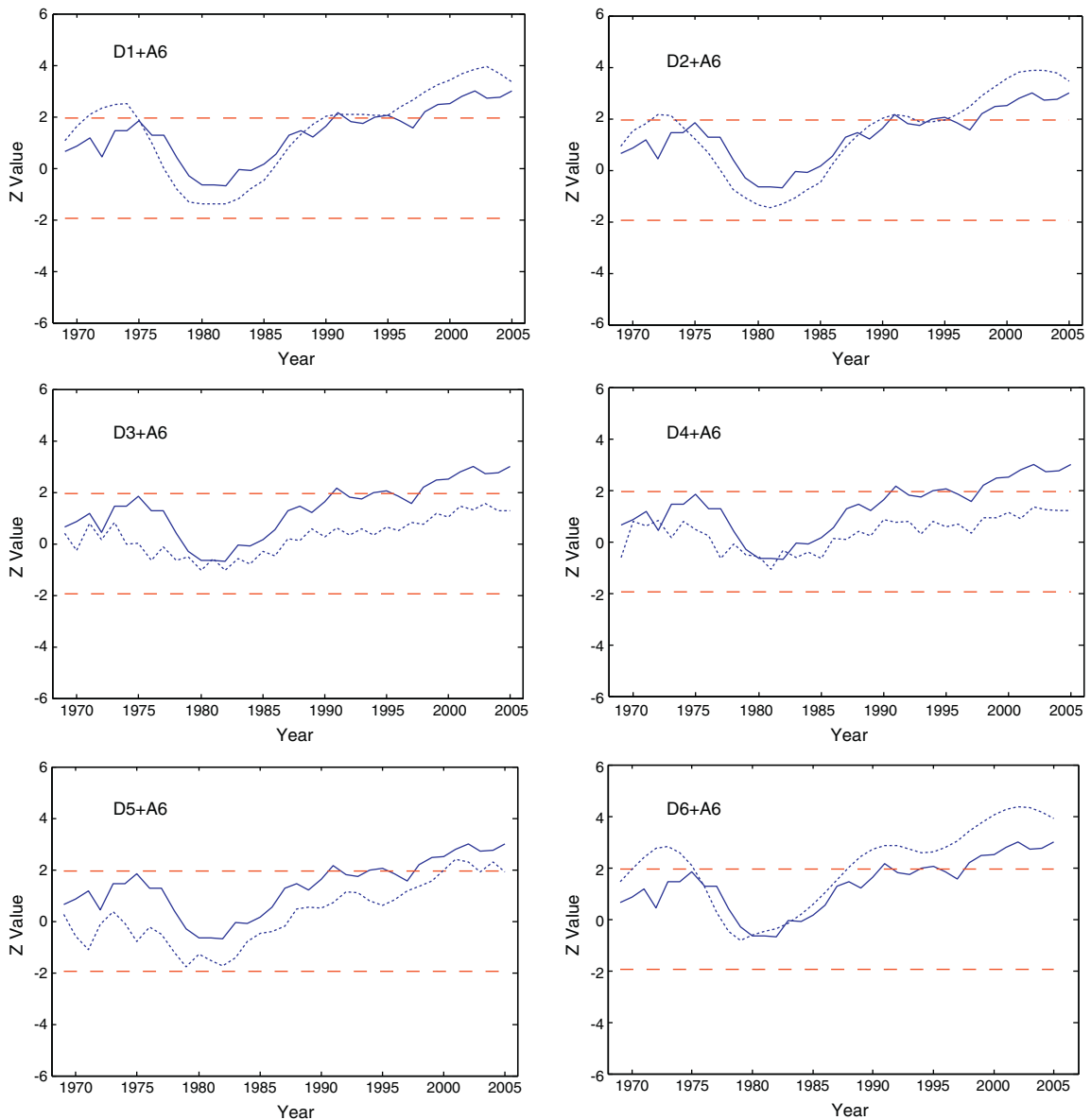


Fig. 4. Station Harrow's monthly temperature series and its decomposition via the DWT using db3 wavelet, into six levels (D1–D6 and A6).



**Fig. 5.** Sequential Mann–Kendall graphs of station Harrow's monthly temperature data. The progressive trend lines of the original data are represented by the solid lines and the trend lines of the detail components (with their approximation added) are represented by the dashed line. The upper and lower dashed lines represent the confidence limits ( $\alpha = 5\%$ ). For this station, D1 and D2 are considered the most dominant periodic components because of the harmony of their progressive trend lines and their MK Z-values being close to that of the original data.

1955–2005. A more recent assessment by [Statistics Canada \(2011\)](#) also showed that over the period of 1948 to 2009 there was an increase of 1.4 °C in the mean annual temperature in Canada. More pertinent to our study, the Great Lakes and St. Lawrence and the Northeastern Forest (which covers most of Ontario and Quebec) regions experienced an increasing trend in the mean temperature departure from 1961 to 1990 normal – the mean temperature trend increased up to 0.9 °C over the period 1948–2009 ([Statistics Canada, 2011](#)).

In our study, we also discovered that all the MK Z-values of the annual data are greater than +1.96, which imply that there are significant positive trends. The annual temperature

data were decomposed into either 4 or 5 levels. For stations Harrow and Vineland, the D3 components – which correspond to the 8-year periodicity – were considered the most dominant periodic modes that affect the temperature trends in the annual data ([Table 6](#)). The MK Z-values of the D3 components for these stations are the closest to the MK Z-values of their corresponding original data. Furthermore, the sequential MK graphs of the D3 components are also harmonious with those of the original data (see [Fig. 7](#) for example). For station Belleville, the 32-year periodic mode is the most dominant one, and for stations Peterborough and Val d'Or, it is the 16-year mode. To summarize, the increasing

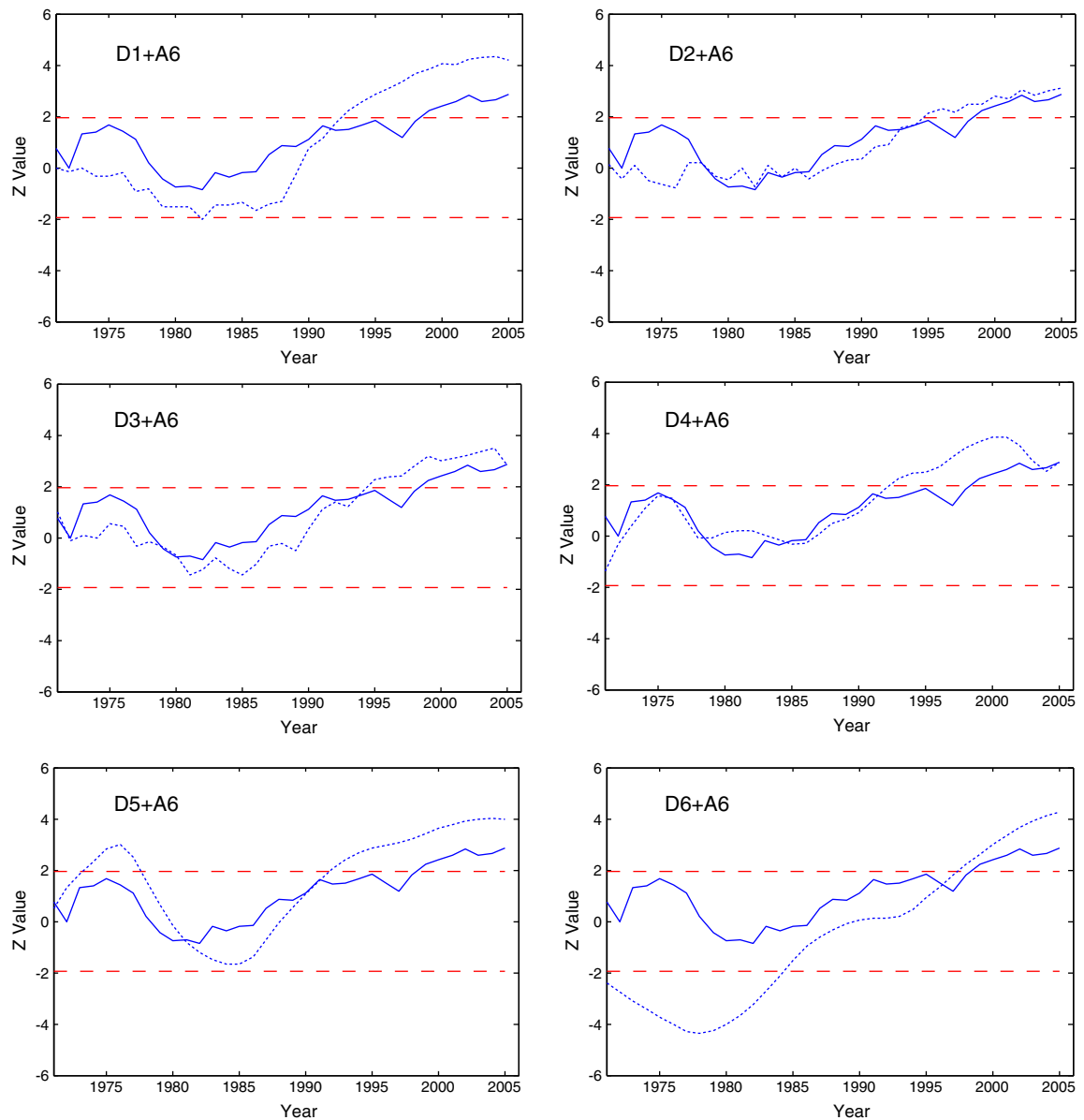


**Fig. 6.** Sequential Mann–Kendall graphs of station Harrow's seasonally-based temperature data. The progressive trend lines of the original data are represented by the solid lines and the trend lines of the detail components (with their approximation added) are represented by the dashed lines.

trends in the annual mean temperature during 1954–2008 over southern parts of Quebec and Ontario are affected by periodicities between 8 and 32 years.

Since all annual temperature data in this study showed significant trend values, each season was analyzed separately in order to investigate the seasons that contribute to the warming trend over the study area to a greater extent compared to the other seasons.

##### 5.5. Winter temperature data analysis

Several studies have mentioned that winter experiences significant warming trends in the northern hemisphere and in countries such as Canada and the USA (e.g. Jones and Briffa,

1992; Lu et al., 2005; Vincent et al., 2007; Mohsin and Gough, 2010; Bukovsky, 2012). In this study, it is also observed that winter warming is very apparent because, apart from station Val d'Or, all stations show significant positive trends with MK Z-values that are relatively high. Even for Val d'Or, the winter MK Z-value (+1.80) is also just slightly below +1.96.

The winter time series for station Harrow was decomposed into three levels, and the remaining time series were decomposed into five levels (Table 7). Table 7 summarizes the MK Z-values for the winter temperature data decompositions, as well as the periodic modes that are considered most dominant for winter temperature trends. The winter temperature trends for station Harrow are mostly affected by the 2-year and 8-year periodicities (i.e. D1 and D3 detail components) (Fig. 8).

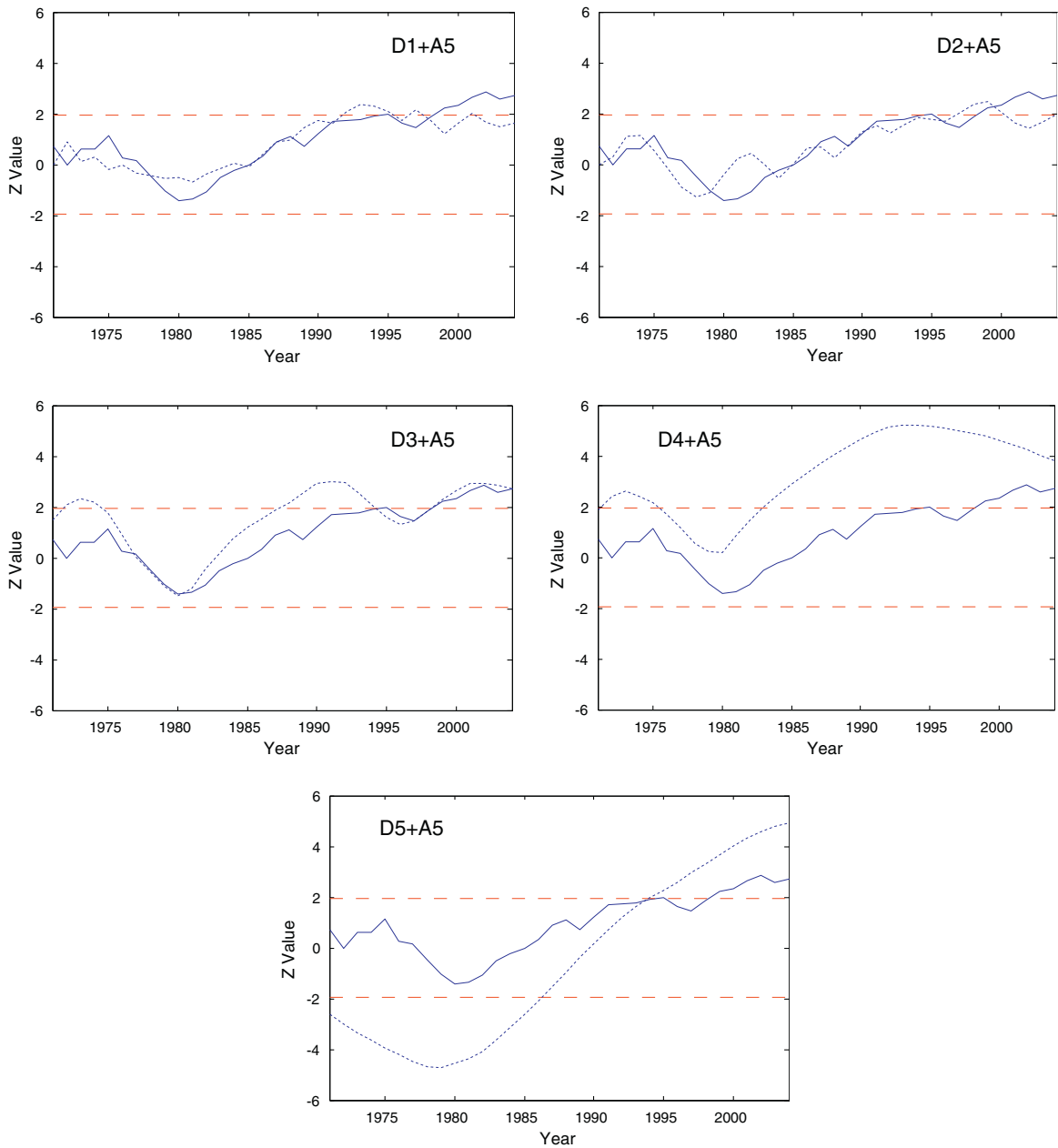


**Fig. 7.** Sequential Mann–Kendall graphs of station Harrow's annual temperature data. The progressive trend lines of the original data are represented by the solid lines and the trend lines of the detail components (with their approximation added) are represented by the dashed lines. The upper and lower dashed lines represent the confidence limits ( $\alpha = 5\%$ ). For this station, D3, which represents the 8-year time scale, is the most dominant periodicity for trends.

Peterborough station's most dominant periodicity is the 16-year periodic mode (i.e. D4 component with approximation). For station Vineland, D3 and D4 (with approximation) have MK Z-values that are closest to that of the original data ( $Z = +1.97$ ); as well, graphically, D3 and D4 have good sequential harmony with the original data compared to the rest (Fig. 9). Therefore, it can be said that for station Vineland, the 8-year and 16-year periodic components are considered the most dominant for trends in winter temperature data. Similarly, for station Belleville, the D3 component (8-year

periodic mode) has the closest MK Z-value ( $Z = +1.64$ ) to that of the original data ( $Z = +2.60$ ) with better sequential MK compared to other detail components.

Similar to the results of the annual data analysis, the trends in winter temperature warming are also mostly affected by periodic events of 8 years or greater (up to 16 years). These important periodicities may be related to the variability of the large-scale atmospheric circulations such as the North Atlantic Oscillation (NAO), El-Niño Southern Oscillation (ENSO), and Pacific North American (PNA) oscillation. The NAO is a very

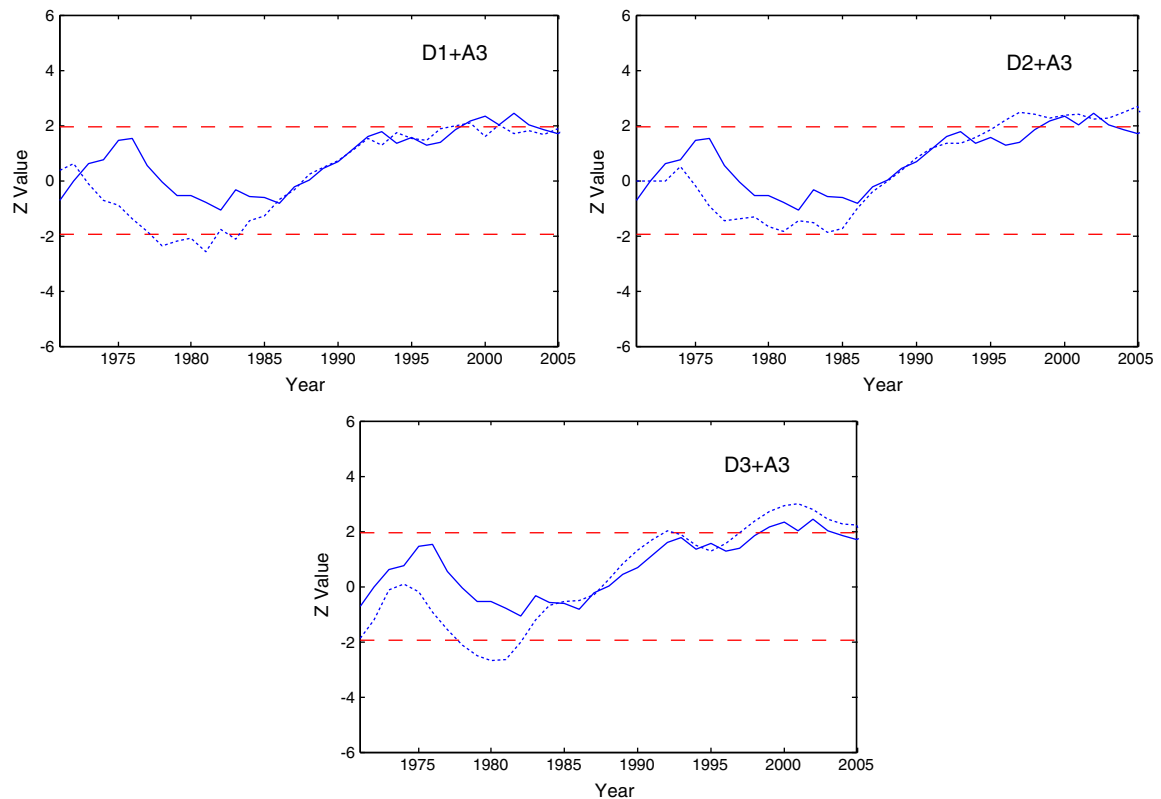


**Fig. 8.** Sequential Mann-Kendall graphs of station Harrow's winter temperature data. The progressive trend lines of the original data are represented by the solid lines and the trend lines of the detail components (with their approximation added) are represented by the dashed lines. The upper and lower dashed lines represent the confidence limits ( $\alpha = 5\%$ ). For this station, D1 and D3 components were considered the most dominant periodicities for trends.

important large-scale climatic phenomenon in the northern hemisphere (Anctil and Coulibaly, 2004), especially in central and eastern Canada (Damyanov et al., 2012) and is known to strongly exhibit inter-annual to decadal variability with some of its major peaks centered around 2.1, 8 and 24 years (Cook et al., 1998; Anctil and Coulibaly, 2004). Many studies have also found a strong relationship between the NAO and temperature trends (e.g. for Canada: Wettstein and Mearns, 2002; Bonsal et al., 2006; Damyanov et al., 2012). Positive phases of the NAO cycles tend to cause above normal temperatures. The NAO has been in its positive phase since 1970 (Anctil and Coulibaly, 2004), which could contribute to the significant positive trends observed in this study. Hasanian (2001) also mentioned that the NAO variability is strongest during winter, and that the winter NAO cycle is very effective in affecting temperature variability in mid-latitude areas. Other important large-scale climate circulations such as the ENSO and the PNA oscillation also affect the temperature trends (e.g. Bonsal and Shabbar, 2011). One of the causes of the variability of these large-scale climate circulations is related to solar activities, which are frequently manifested as the 11-year solar period (Prokoph et al., 2012). It has been indicated that there are similar variabilities between surface temperatures and the 11-year solar cycle, which may contribute to the observed global warming to some extent (e.g. Lassen, 1991; Erlykin et al., 2009; de Jager et al., 2010; Solheim et al., 2011). The 11-year solar period could also be applicable in our study since the periodicity

is in between 8- and 16-year modes, which are the most commonly observed as the dominant periodicities affecting the temperature trends.

#### 5.6. Spring temperature data analysis

All stations showed positive MK Z-values with only Vineland experiencing a significant trend. The number of decomposition levels via the DWT for each spring temperature data can be seen in Table 8. As shown in Table 8, the D3 (8-year periodicity) component is the one considered most influential for the spring temperature trend in stations Harrow and Peterborough. For stations Vineland, it is the D2 (4-year periodicity), and for stations Belleville and Val d'Or, the D1 (2-year periodicity) is the most dominant for trend.

An example of spring temperature analysis using the DWT and sequential MK analysis is shown in Fig. 10. It is noted that for station Harrow, the dominant 8-year periodicity is consistent with the observations in the winter and annual data. Even though most of the trend values for spring temperature are not significant, all of the trend values are positive. It is also possible that positive and negative trends may cancel each other out at some point over the study period. Determining the most dominant periodic modes for trends is still deemed important because it helps to understand the periodicities that characterize the trends in spring temperature.

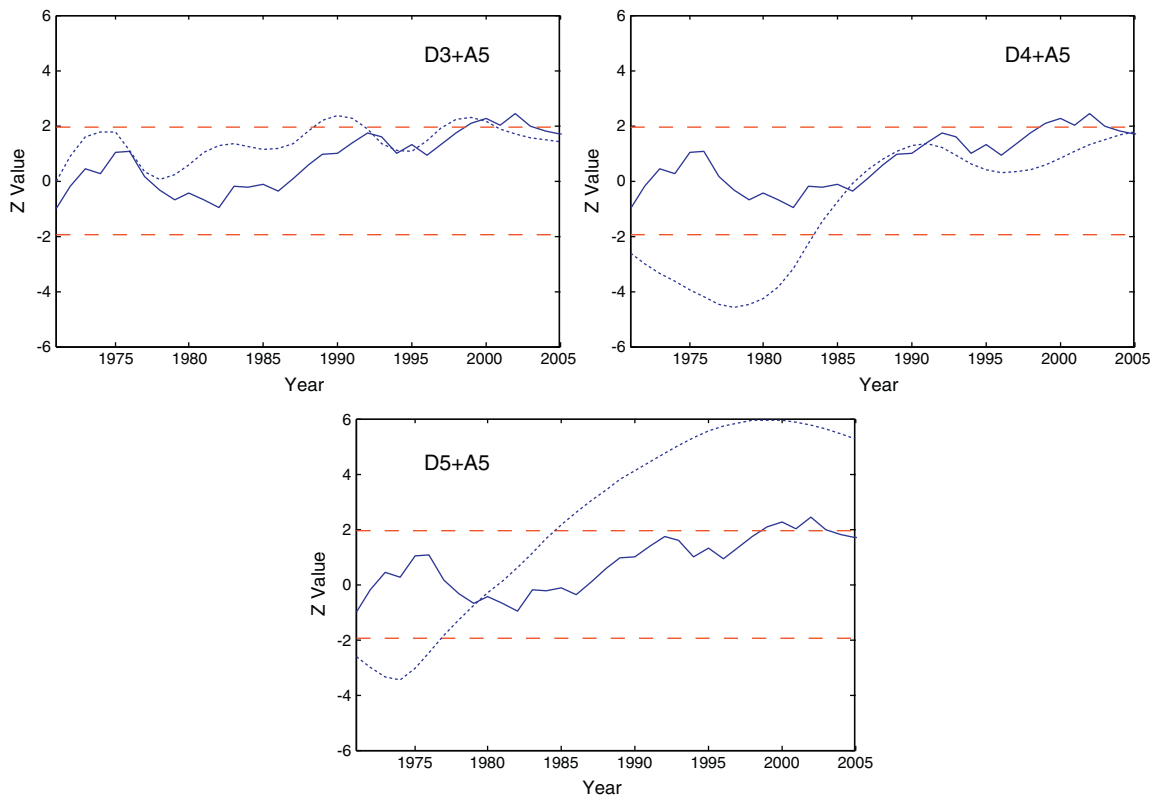


**Fig. 9.** A comparison of the sequential Mann–Kendall graphs among D3, D4, and D5 (all with approximation added) of station Vineland's winter temperature data. The progressive trend lines of the original data are represented by the solid lines and the trend lines of the detail components are represented by the dashed lines. The upper and lower dashed lines represent the confidence limits ( $\alpha = 5\%$ ).

The finding in our study showing that most stations did not experience a significant temperature increase for the spring season is somewhat inconsistent with the findings from several studies that analyzed seasonal temperatures in mid-latitude areas (including Canada). Zhang et al. (2000) found that spring experienced the greatest warming in southern Canada. Vincent et al. (2007) also emphasized a significant warming in the spring in southern Canada during the period 1953–2005. This disagreement could be caused by the differences in the geographical locations of the stations used and the time period chosen. The stations included in our study are only concentrated around the most south-westerly parts of Ontario and Quebec. Even so, these differences suggest that it is important to conduct a more localized assessment on trends in temperature.

### 5.7. Summer temperature data analysis

In addition to winter, it has also been pointed out by other Canadian studies that summer also experiences significant warming, although sometimes to a lesser extent compared to winter warming (e.g. Vincent et al., 2007; Mohsin and Gough, 2010). In this study, all stations are experiencing significant positive summer temperature trends, except for Peterborough station (Table 9). Table 9 summarizes the decomposition of the summer temperature time series and the MK Z-values of the different detail components, and the details plus their respective approximations. As can be seen in Table 9, the most dominant

periodicities for trends are the D3 and D4 components, which represent the 8-year and 16-year time periodicities, respectively.

Fig. 11 shows an example of the sequential MK analysis on Harrow's summer temperature series, and how the D2 and D3 components (with approximation) show the most harmonious trend lines as compared to that of the original data. It is interesting to note that the most dominant periodicities in stations Harrow and Peterborough are again consistent with the results from their annual and winter data analysis: D3 for Harrow and D4 for Peterborough. It is again seen that in the summer data analysis, the most influential periodic modes that affect the trends are made up of multi-year and decadal events (between 8 and 16 years). The agreement found in annual, winter, and summer temperature trends could suggest that the positive trends in the annual temperature over the study area may be contributed mostly by the increase in winter and summer temperatures. Several causes of winter and summer warming trends in Canada have been investigated in past studies. For example, Vincent et al. (2007) concluded that winter warming in Canada is due to an increase in dewpoint and specific humidity. More specifically, Prokoph and Patterson (2004) and Adamowski and Prokoph (2013) associated winter warming in urban settings in eastern Ontario with the heat island effect. Summer warming is also associated with the increase in air moisture, especially around the Great Lakes and St. Lawrence areas (Vincent et al., 2007).

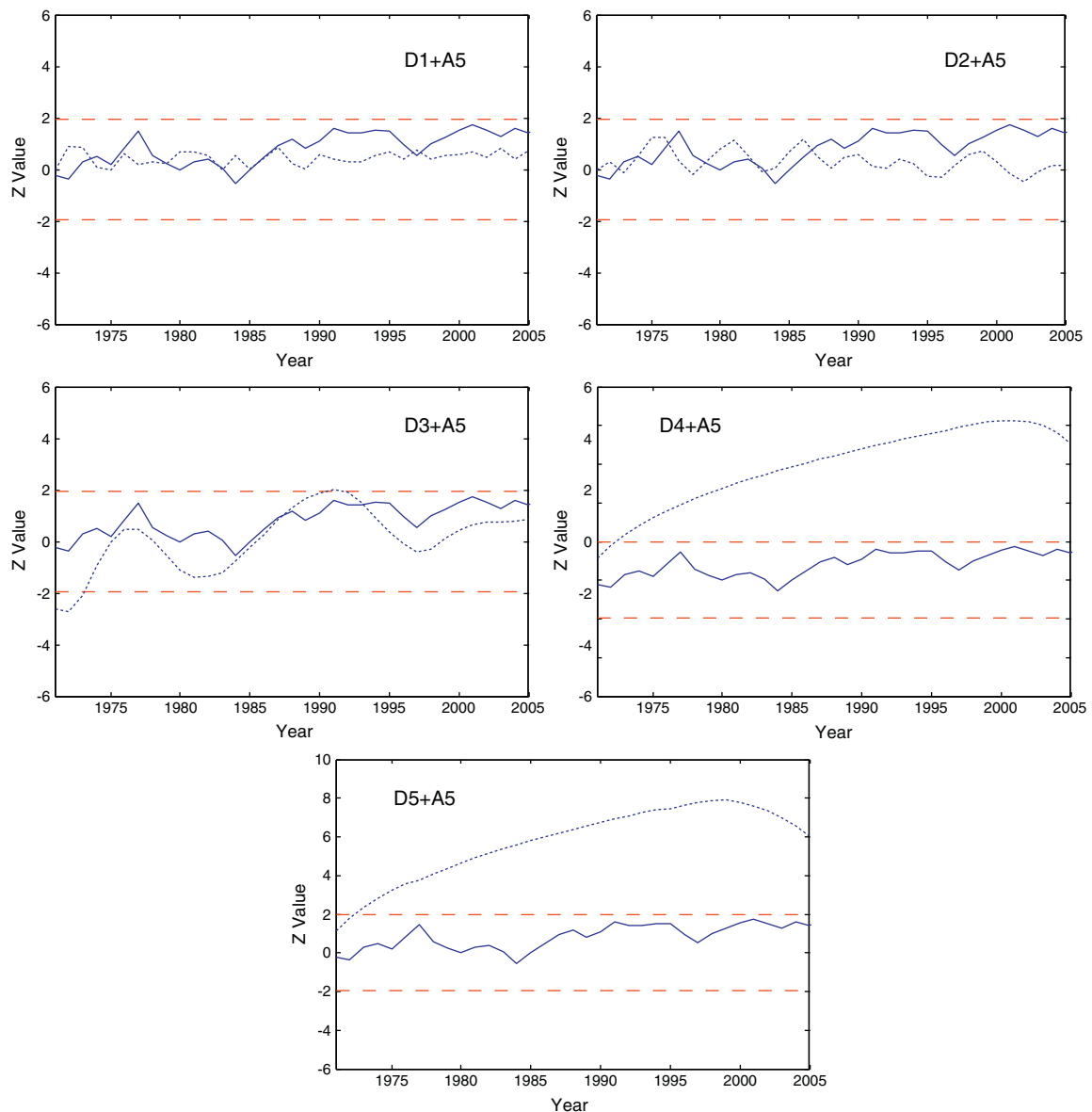


**Fig. 10.** Sequential Mann–Kendall graphs of station Harrow's spring temperature data. The progressive trend lines of the original data are represented by the solid line and the trend lines of the detail components (with their approximation added) are represented by the dashed lines. The upper and lower dashed lines represent the confidence limits ( $\alpha = 5\%$ ). For this station, the D3 component was considered the most dominant periodicity for trends.

### 5.8. Autumn temperature data analysis

Although it is noted that all the MK Z-values for autumn temperatures are positive, autumn is the only season in which none of the stations explored in this study experience significant trends (Table 10). This observation is not surprising as it is in agreement with several studies where autumn has the least number of stations with significant warming (see for example: Vincent et al., 2007). It can be seen in Table 10 that the dominant periodic components affecting the trends in autumn temperature are slightly different from station to station. For stations Harrow and Peterborough, it is the D2 (4-year mode); for station Vineland, it is the D3 (8-year mode);

and for stations Belleville and Val d'Or, it is the D1 (2-year mode). Again, these important periodic modes may have coincided with some of the major peaks of the NAO cycle (i.e. 2 and 8 years). Although the NAO is not the only factor that influences the temperature variability over the study area, it can be considered an important factor.

An example of autumn temperature data decomposition and sequential MK analysis is given in Fig. 12. Generally, the trends in autumn temperatures are characterized by 2- to 8-year periodicities (Table 10), which are inconsistent with the results obtained from annual, winter, and summer data analyses where most trends are influenced by periodicities that are greater than eight years. This observation could suggest

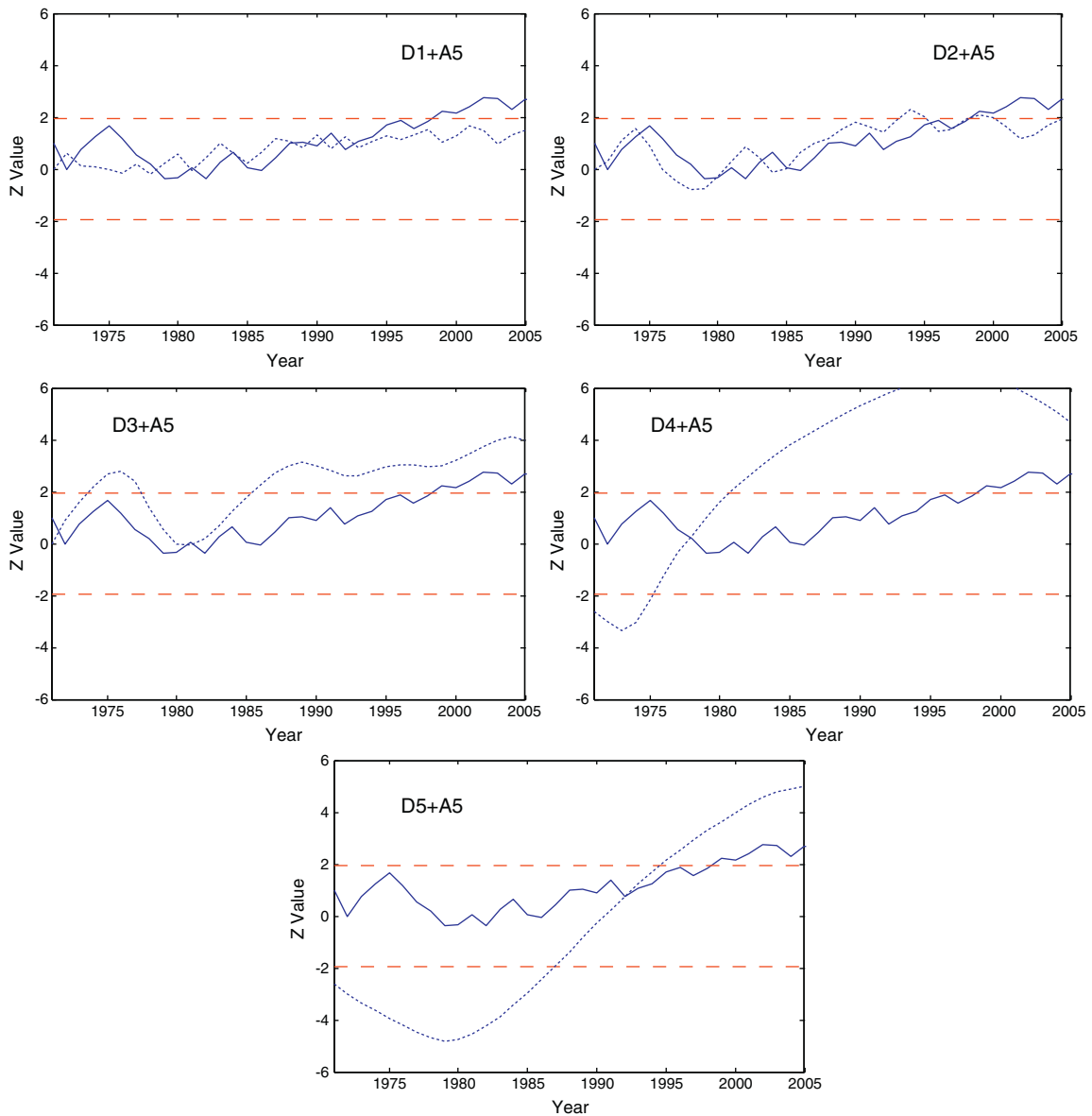


**Fig. 11.** Sequential Mann–Kendall graphs of station Harrow's summer temperature data. The progressive trend lines of the original data are represented by the solid lines and the trend lines of the detail components (with their approximation added) are represented by the dashed lines. The upper and lower dashed lines represent the confidence limits ( $\alpha = 5\%$ ). For this station, D2 and D3 components were chosen to be the most dominant periodicities for trends.

that autumn has minimal contribution towards the warming trends observed in the annual temperature data over the study area.

## 6. Conclusions and recommendations

Surface air temperature trends from a total of five stations located in Ontario and Quebec were analyzed using the WT and the MK trend test. The use of the DWT prior to applying the MK test in analyzing temperature trends was found to be very useful in this study. The original data were decomposed into a series of their detail and approximation components and then they were tested with the MK test. By doing so, we were able to obtain information about the periodic mode(s)

considered important in affecting the observed trends of a specific dataset.

The observations and findings of this study reveal that southern parts of Ontario and Quebec are experiencing warming trends in temperature. The use of monthly and seasonally based data in our study was found to be useful in determining the influence of higher-frequency events (short-term periodic modes) on the observed trends. Warming trends in the monthly data are affected by high-frequency periodicities ranging from 2 to 4 months, which may have masked the effect of the longer-time scales (lower frequency components). Annual periodicities are found to affect the trends in seasonally-based data.

The analysis of the lower-resolution data (i.e. annual, winter, spring, summer, and autumn) revealed that low-

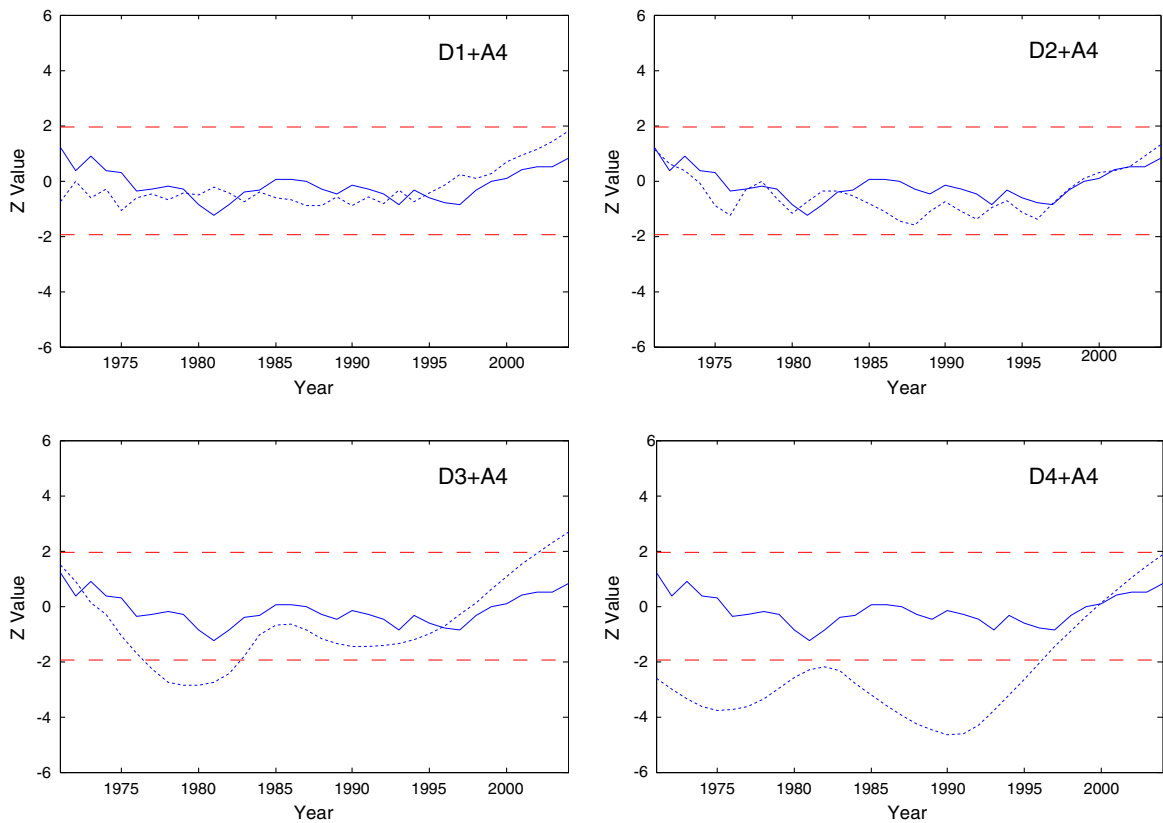


**Fig. 12.** Sequential Mann-Kendall graphs of station Harrow's autumn temperature data. The progressive trend lines of the original data are represented by the solid lines and the trend lines of the detail components (with their approximation added) are represented by the dashed lines. The upper and lower dashed lines represent the confidence limits ( $\alpha = 5\%$ ). For this station, the D2 component, which represents the 4-year time mode, was considered the most dominant periodicity for trends.

frequency periodicities were more dominant in affecting the temperature trends. For annual data, the most important periodic modes that affect their trends are made up of multi-year and decadal events. Wu et al. (2007) demonstrated the superior performance of the multi-decadal trend model in capturing the variability and change in the annual global surface air temperature anomaly (GSTA) for the period 1961–1990. The rate of change in temperature using the multi-decadal trend model was higher compared to the other models, but the longer time scales were found to be more reliable when assessing trends of GSTA. Similarly, the results of the annual data analysis in the present study also revealed that the trends were affected by the higher time-scale components mostly between 8 and 16 years. These time scales explain the variability associated with the annual surface air temperature over southern Quebec and Ontario.

From the seasonal point of analysis, winter and summer are experiencing the most uniform trends in temperature, where all the sites are experiencing significant positive trends (except for Val d'Or's winter data). The results of the winter and summer analysis are also the most consistent with those of the annual data, in which most of the dominant periodic components affecting the trends are also between 8 and 16 years. Based on the findings of this study, it can be suggested that long-term trends in the temperature data over

southern Quebec and Ontario may be due to winter and summer warming. Some possible causes of winter and summer warming that have been identified in previous studies are: increases in dewpoint, air moisture, and humidity (Vincent et al., 2007), and the influence of urban heat island effects (Prokoph and Patterson, 2004).

The relationships between the temperature trends over the study area and large-scale climate circulations important for Canadian climate (e.g. the NAO, ENSO) can be quantified in future studies using correlation analysis. The findings of the present study have established the baseline information about the important periodicities that affect the temperature trends; this can then be incorporated in the future when analyzing the linkages between temperature trends in southern Ontario and Quebec, and different climatic phenomena.

Finally, it would also be very useful to include more stations (perhaps with longer data records) in future studies to obtain more representative results for the whole provinces. However, suitable interpolation methods to fill the missing records found in many stations have to be carefully determined in order to minimize the errors associated with interpolations. In this study, only five stations were included because they are the only ones in our study area that have complete records (with no missing values) for 40 years.

## Acknowledgments

This study was funded by a NSERC Discovery Grant held by Jan Adamowski, as well as a Liliane and David M. Stewart Foundation Scholarship held by Deasy Nalley.

## References

- Adamowski, K., Bougadis, J., 2003. Detection of trends in annual extreme rainfall. *Hydrol. Processes* 17 (18), 3547–3560.
- Adamowski, J., Prokoph, A., 2013. Assessing the impacts of the urban heat island effect on streamflow patterns in Ottawa. *Canada. J. Hydrol.* 496, 225–237.
- Adamowski, K., Prokoph, A., Adamowski, J., 2009. Development of a new method of wavelet aided trend detection and estimation. *Hydrol. Processes* 23 (18), 2686–2696.
- Anctil, F., Coulibaly, P., 2004. Wavelet analysis of the interannual variability in southern Québec streamflow. *J. Clim.* 17 (1), 163–173.
- Baliunas, S., Frick, P., Sokoloff, D., Soon, W., 1997. Time scales and trends in the central England temperature data (1659–1990): a wavelet analysis. *Geophys. Res. Lett.* 24 (11), 1351–1354.
- Bonsal, B., Shabbar, A., 2011. Large-scale climate oscillations influencing Canada, 1900–2008. *Canadian Biodiversity: Ecosystem Status and Trends 2010. Technical Thematic Report No. 4. Canadian Councils of Resource Ministers, Ottawa, ON* (iii + 15 p. <http://www.biodivcanada.ca/default.asp?lang=En&nav=137E1147-0> [accessed 25 June 2012]).
- Bonsal, B.R., Prowse, T.D., Duguay, C.R., Lacroix, M.P., 2006. Impacts of large-scale teleconnections on freshwater-ice break/freeze-up dates over Canada. *J. Hydrol.* 330 (1–2), 340–353.
- Bukovsky, M.S., 2012. Temperature trends in the NARCCAP regional climate models. *J. Clim.* 25, 3985–3991 <http://dx.doi.org/10.1175/JCLI-D-11-00588.1>.
- Burn, D.H., Hag Elnur, M.A., 2002. Detection of hydrologic trends and variability. *J. Hydrol.* 255 (1–4), 107–122.
- Chaouche, K., Neppel, L., Dieulin, C., Pujol, N., Ladouche, B., Martin, E., Salas, D., Caballero, Y., 2010. Analyses of precipitation, temperature and evapotranspiration in a French Mediterranean region in the context of climate change. *C. R. Geosci.* 342 (3), 234–243.
- Chou, C.-M., 2007. Applying multi-resolution analysis to differential hydrological grey models with dual series. *J. Hydrol.* 332 (1–2), 174–186.
- Cook, E.R., D'Arrigo, R.D., Briffa, K.R., 1998. A reconstruction of the North Atlantic Oscillation using tree-ring chronologies from North America and Europe. *Holocene* 8 (1), 9–17.
- Craigmile, P.F., Guttorp, P., Percival, D.B., 2004. Trend assessment in a long memory dependence model using the discrete wavelet transform. *Environmetrics* 15 (4), 313–335.
- Damyantov, N.N., Matthews, H.D., Mysak, L.A., 2012. Observed decreases in the Canadian outdoor skating season due to recent winter warming. *Environ. Res. Lett.* 7 (1), 014028.
- de Artigas, M.Z., Elias, A.G., de Campra, P.F., 2006. Discrete wavelet analysis to assess long-term trends in geomagnetic activity. *Phys. Chem. Earth.* 31 (1–3), 77–80.
- de Jager, C., Duhau, S., van Geel, B., 2010. Quantifying and specifying the solar influence on terrestrial surface temperature. *J. Atmos. Sol.-Terr. Phys.* 72, 926–937.
- Dietz, E.J., Killeen, T.J., 1981. A nonparametric multivariate test for monotone trend with pharmaceutical applications. *J. Am. Stat. Assoc.* 76 (373), 169–174.
- Domroes, M., El-Tantawi, A., 2005. Recent temporal and spatial temperature changes in Egypt. *Int. J. Climatol.* 25 (1), 51–63.
- Dong, X., Nyren, P., Patton, B., Nyren, A., Richardson, J., Maresca, T., 2008. Wavelets for agriculture and biology: a tutorial with applications and outlook. *BioScience* 58 (5), 445–453.
- Drago, A.F., Boxall, S.R., 2002. Use of the wavelet transform on hydro-meteorological data. *Phys. Chem. Earth.* 27 (32–34), 1387–1399.
- Erlaykin, A.D., Sloan, T., Wolfendale, A.W., 2009. Solar activity and the mean global temperature. *Environ. Res. Lett.* 4 (2009), 014006.
- Fan, X.-H., Wang, M.-B., 2011. Change trends of air temperature and precipitation over Shanxi Province, China. *Theor. Appl. Climatol.* 103 (3–4), 519–531.
- Farge, M., 1992. Wavelet transforms and their applications to turbulence. *Annu. Rev. Fluid Mech.* 24, 395–457.
- Franzke, C., 2010. Long range dependence and climate noise characteristics of Antarctic temperature data. *J. Clim.* 23, 6074–6081.
- Gough, W.A., 2008. Theoretical considerations of day-to-day temperature variability applied to Toronto and Calgary, Canada data. *Theor. Appl. Climatol.* 94 (1–2), 97–105.
- Hamed, K.H., Rao, A.R., 1998. A modified Mann–Kendall trend test for autocorrelated data. *J. Hydrol.* 204 (1–4), 182–196.
- Hasanean, H.M., 2001. Fluctuations of surface air temperature in the Eastern Mediterranean. *Theor. Appl. Climatol.* 68 (1–2), 75–87.
- Hirsch, R.M., Slack, J.R., 1984. A nonparametric trend test for seasonal data with serial dependence. *Water Resour. Res.* 20 (6), 727–732.
- IPCC, 2007. *Climate change 2007: the fourth IPCC scientific assessment*. In: Parry, M.L., Canziani, O.F., Palutikof, J.P., van der Linden, P.J., Hanson, C.E. (Eds.), Intergovernmental Panel on Climate Change. Cambridge University Press, Cambridge, United Kingdom and New York, NY, USA.
- Jones, P.D., Briffa, K.R., 1992. Global surface air temperature variations during the twentieth century: part 1, spatial, temporal and seasonal details. *Holocene* 2 (2), 165–179.
- Jones, P.D., Moberg, A., 2003. Hemispheric and large-scale surface air temperature variations: an extensive revision and an update to 2001. *J. Clim.* 16, 206–223.
- Jung, H.-S., Choi, Y., Oh, J.-H., Lim, G.-H., 2002. Recent trends in temperature and precipitation over South Korea. *Int. J. Climatol.* 22 (11), 1327–1337.
- Kadioglu, M., 1997. Trends in surface air temperature data over Turkey. *Int. J. Climatol.* 17 (5), 511–520.
- Kahya, E., Kalayci, S., 2004. Trend analysis of streamflow in Turkey. *J. Hydrol.* 289 (1–4), 128–144.
- Kallache, M., Rust, H.W., Kropp, J., 2005. Trend assessment: applications for hydrology and climate research. *Nonlinear Process. Geophys.* 12 (2), 201–210.
- Karaburun, A., Demirci, A., Kara, F., 2011. Analysis of spatially distributed annual, seasonal and monthly temperatures in Istanbul from 1975 to 2006. *World Appl. Sci. J.* 12 (10), 1662–1675.
- Kendall, M.G., 1975. *Rank Correlation Methods*. Charles Griffin, London.
- Kravchenko, V.O., Evtushevsky, O.M., Grytsai, A.V., Milinevsky, G.P., 2011. Decadal variability of winter temperatures in the Antarctic Peninsula region. *Antarct. Sci.* 23 (6), 614–622.
- Labat, D., Goddérès, Y., Probst, J.L., Guyot, J.L., 2004. Evidence for global runoff increase related to climate warming. *Adv. Water Resour.* 27 (6), 631–642.
- Lassen, K., 1991. Long-term variations in solar activity and their apparent effect on the earth's climate. <http://www.tmgnow.com/repository/solar/lassen1.html> (accessed 25 July 2012).
- Lau, K.M., Weng, H., 1995. Climate signal detection using wavelet transform: how to make a time series sing. *Bull. Am. Meteorol. Soc.* 76 (12), 2391–2402.
- Lim, Y.-H., Lye, L.M., 2004. Wavelet analysis of tide-affected low streamflows series. *J. Data Sci.* 2, 149–163.
- Lindsay, R.W., Percival, D.B., Rothrock, D.A., 1996. The discrete wavelet transform and the scale analysis of the surface properties of sea ice. *IEEE Trans. Geosci. Remote Sens.* 34 (3), 771–787.
- Lu, Q., Lund, R., Seymour, L., 2005. An update of U.S. temperature trends. *J. Clim.* 18, 4906–4914.
- Ludwig, W., Serrat, P., Csmat, L., Garcia-Esteves, J., 2004. Evaluating the impact of the recent temperature increase on the hydrology of the Têt River (Southern France). *J. Hydrol.* 289 (1–4), 204–221.
- Lund, R., Seymour, L., Kafadar, K., 2001. Temperature trends in the United States. *Environmetrics* 12 (7), 673–690.
- Ma, J., Xue, J., Yang, S., He, Z., 2003. A study of the construction and application of a Daubechies wavelet-based beam element. *Finite Elem. Anal. Des.* 39, 965–975.
- Makokha, G.L., Shisanya, C.A., 2010. Trends in mean annual minimum and maximum near surface temperature in Nairobi city, Kenya. *Adv. Meteorol.* 6. <http://dx.doi.org/10.1155/2010/676041> (Article ID 676041).
- Mann, H.B., 1945. Nonparametric tests against trend. *Econometrica* 13 (3), 245–259.
- Mekis, É., Vincent, L.A., 2011. An overview of the second generation adjusted daily precipitation dataset for trend analysis in Canada. *Atmosphere-Ocean* 49 (2), 163–177.
- Mimikou, M.A., Baltas, E., Varanou, E., Pantazis, K., 2000. Regional impacts of climate change on water resources quantity and quality indicators. *J. Hydrol.* 234 (1–2), 95–109.
- Mishra, A.K., Singh, V.P., 2010. Changes in extreme precipitation in Texas. *J. Geophys. Res.* 115 (D14), D14106.
- Moberg, A., Sonechkin, D.M., Holmgren, K., Datsenko, N.M., Karlen, W., 2005. Highly variable Northern Hemisphere temperatures reconstructed from low- and high-resolution proxy data. *Nature* 433 (7026), 613–617.
- Mohsin, T., Gough, W., 2010. Trend analysis of long-term temperature time series in the Greater Toronto Area (GTA). *Theor. Appl. Climatol.* 101 (3), 311–327.
- Nalley, D., Adamowski, J., Khalil, B., 2012. Using discrete wavelet transforms to analyze trends in streamflow and precipitation in Quebec and Ontario (1954–2008). *J. Hydrol.* 475, 204–228.
- Nicholls, R.J., Tol, R.S.J., 2006. Impacts and responses to sea-level rise: a global analysis of the SRES scenarios over the twenty-first century. *Philos. Trans. R. Soc. A* 364 (1841), 1073–1095.
- Nicholls, N., Gruza, G.V., Jouzel, J., Karl, T.R., Ogallo, L.A., Parker, D.E., 1996. Observed climate variability and change. In: Houghton, J.T., Filho, L.G.M., Callander, B.A., Harris, N., Kattenberg, A., Maskell, K. (Eds.), *Climate*

- Change 1995: The Science of Climate Change. 132–192. Cambridge University Press, Cambridge, UK.
- Partal, T., 2010. Wavelet transform-based analysis of periodicities and trends of Sakarya basin (Turkey) streamflow data. *River Res. Appl.* 26 (6), 695–711.
- Partal, T., Kahya, E., 2006. Trend analysis in Turkish precipitation data. *Hydrol. Processes* 20, 2011–2026.
- Partal, T., Küçük, M., 2006. Long-term trend analysis using discrete wavelet components of annual precipitations measurements in Marmara region (Turkey). *Phys. Chem. Earth*. 31 (18), 1189–1200.
- Percival, D.B., 2008. Analysis of geophysical time series using discrete wavelet transforms: an overview. In: Donner, R.V., Barbosa, S.M. (Eds.), *Nonlinear Time Series Analysis in the Geosciences – Applications in Climatology, Geodynamics, and Solar-terrestrial Physics*. Springer, Berlin/Heidelberg.
- Pišoft, P., Kalvová, J., Brázdil, R., 2004. Cycles and trends in the Czech temperature series using wavelet transforms. *Int. J. Climatol.* 24 (13), 1661–1670.
- Polyakov, I.V., Bekryaev, R.V., Alekseev, G.V., Bhatt, U.S., Colony, R.L., Johnson, M.A., Maskshat, A.P., Walsh, D., 2003. Variability and trends of air temperature and pressure in the Maritime Arctic, 1875–2000. *J. Clim.* 16 (12), 2067–2077.
- Popivanov, I., Miller, R.J., 2002. Similarity search over time-series data using wavelets. *Proceedings of the 18th IEEE International Conference on Data Engineering*, pp. 212–221.
- Prokoph, A., Patterson, R.T., 2004. Application of wavelet and regression analysis in assessing temporal and geographic climate variability: Eastern Ontario, Canada as a case study. *Atmosphere-Ocean* 43 (2), 201–212.
- Prokoph, A., Adamowski, J., Adamowski, K., 2012. Influence of the 11 year solar cycle on annual streamflow maxima in Southern Canada. *J. Hydrol.* 442–443, 55–62.
- Rebetez, M., Reinhard, M., 2007. Monthly air temperature trends in Switzerland 1901–2000 and 1975–2004. *Theor. Appl. Climatol.* 91 (1–4), 27–34.
- Shrestha, A.B., Wake, C.P., Mayewski, P.A., Dibb, J.E., 1999. Maximum temperature trends in the Himalaya and its vicinity: an analysis based on temperature records from Nepal for the period 1971–94. *J. Clim.* 12 (9), 2775–2786.
- Solheim, J.-K., Stordahl, K., Humlum, O., 2011. Solar activity and Svalbard temperatures. *Adv. Meteorol.* 8. <http://dx.doi.org/10.1155/2011/543146> (Article ID 543146).
- Statistics Canada, 2011. Temperature trends in Canada. *EnviroStats* 5 (1) (Catalogue No. 16-002-X).
- Su, H., Liu, Q., Li, J., 2011. Alleviating border effects in wavelet transforms for nonlinear time-varying signal analysis. *Adv. Electr. Comput. Eng.* 11 (3), 6.
- Torrence, C., Compo, G.P., 1998. A practical guide to wavelet analysis. *Bull. Am. Meteorol. Soc.* 79 (1), 61–78.
- Vincent, L.A., Gullett, D.W., 1999. Canadian historical and homogeneous temperature datasets for climate change analyses. *Int. J. Climatol.* 19 (12), 1375–1388.
- Vincent, L.A., van Wijngaarden, W.A., Hopkinson, R., 2007. Surface temperature and humidity trends in Canada for 1953–2005. *J. Clim.* 20 (20), 5100–5113.
- Vincent, L.A., Milewska, E.J., Hopkinson, R., Malone, L., 2009. Bias in minimum temperature introduced by a redefinition of the climatological day at the Canadian synoptic stations. *J. Appl. Meteorol. Climatol.* 48 (10), 2160–2168.
- Vonesch, C., Blu, T., Unser, M., 2007. Generalized Daubechies wavelet families. *IEEE Trans. Signal Process.* 55 (9), 4415–4429.
- Wang, N., Lu, C., 2009. Two-dimensional continuous wavelet analysis and its application to meteorological data. *J. Atmos. Ocean. Technol.* 27 (4), 652–666.
- Wang, J.Z., Wiederhold, G., Firschein, O., Xin Wei, S., 1998. Content-based image indexing and searching using Daubechies' wavelets. *Int. J. Digit. Libr.* 1 (4), 311–328.
- Wettstein, J.J., Mearns, L.O., 2002. The influence of the North Atlantic–Arctic oscillation on mean, variance, and extremes of temperature in the northeastern United States and Canada. *J. Clim.* 15 (24), 3586–3600.
- Wu, Z., Huang, N.E., Long, S.R., Peng, C.-K., 2007. On the trend, detrending, and variability of nonlinear and nonstationary time series. *Proc. Natl. Acad. Sci. U. S. A.* 104 (38), 14889–14894.
- Yue, S., Pilon, P., Phinney, B., Cavadias, G., 2002. The influence of autocorrelation on the ability to detect trend in hydrological series. *Hydrol. Processes* 16 (9), 1807–1829.

- Zhang, X., Vincent, L.A., Hogg, W.D., Niitsoo, A., 2000. Temperature and precipitation trends in Canada during the 20th century. *Atmos. Ocean* 38 (3), 395–429.



**Deasy Nalley** is currently pursuing her Ph.D. in the Department of Bioresource Engineering, McGill University, Canada. Her current research interests are in the area of trend estimation and analysis of hydrological data using wavelet transforms and the Mann–Kendall trend test.



**Dr. Jan Adamowski** is an Assistant Professor of Hydrology and Water Resources Management in the Department of Bioresource Engineering at McGill University in Canada. At McGill, he is also the Liliane and David M. Stewart Scholar in Water Resources, the Director of the Integrated Water Resources Management Program (which comprises a Master of Science program and an Online Certification Program), and the Associate Director of the Brace Centre for Water Resources Management. Dr. Adamowski's teaching and research activities revolve around statistical hydrology and integrated and adaptive water resources management.



**Dr. Bahaa Khalil** is a Postdoctoral Fellow in the Department of Bioresource Engineering at McGill University in Canada. Dr. Khalil's research activities revolve around assessment and redesign of environmental monitoring networks, water quality assessment, statistical hydrology, hydrologic and water quality modeling. He has 18 years of research experience with 50 publications in peer-reviewed journals, conference proceedings and technical reports.



**Dr. Bogdan Ozga-Zielinski** is an Assistant Professor in the Division of Protection and Development of Environment, in the Faculty of Environmental Engineering at the Warsaw University of Technology, where he lectures in hydrology. At the same time, he is the Head of the Centre of Hydrology at the Institute of Meteorology and Water Management-National Research Institute of Poland, where he is responsible for the coordination of water resources and applied hydrology research and international co-operation in hydrology with the World Meteorological Organization and other European entities. His main fields of interest

are flood frequency analysis and mathematical modeling of hydrological processes.